


Glutamate dehydrogenase in “Liverworld”—A study in selected species to explore a key enzyme of plant primary metabolism in Marchantiophyta

Martina Brambilla¹ | Giorgio Chiari¹ | Mauro Commisso² | Luca Nerva³ |
 Rita Musetti⁴ | Alessandro Petraglia¹ | Francesca Degola¹ 

¹Department of Chemistry, Life Science and Environmental Sustainability, University of Parma, Parma, Italy

²Department of Biotechnology, University of Verona, Verona, Italy

³Council for Agricultural Research and Economics – Research Centre for Viticulture and Enology (CREA-VE), Conegliano, Italy

⁴Department of Land, Environment, Agriculture and Forestry, University of Padova, Padova, Italy

Correspondence

Francesca Degola, Department of Chemistry, Life Science and Environmental Sustainability, University of Parma, Parma, Italy.
 Email: francesca.degola@unipr.it

Edited by S. de Vries

Abstract

In plants, glutamate dehydrogenase (GDH) is an ubiquitous enzyme that catalyzes the reversible amination of 2-oxoglutarate in glutamate. It contributes to both the amino acid homeostasis and the management of intracellular ammonium, and it is regarded as a key player at the junction of carbon and nitrogen assimilation pathways. To date, information about the GDH of terrestrial plants refers to a very few species only. We focused on selected species belonging to the division Marchantiophyta, providing the first panoramic overview of biochemical and functional features of GDH in liverworts. Native electrophoretic analyses showed an isoenzymatic profile less complex than what was reported for *Arabidopsis thaliana* and other angiosperms: the presence of a single isoform corresponding to an α -homohexamer, differently prone to thermal inactivation on a species- and organ-basis, was found. Sequence analysis conducted on amino acid sequences confirmed a high similarity of GDH in modern liverworts with the GDH2 protein of *A. thaliana*, strengthening the hypothesis that the duplication event that gave origin to *GDH1*-homolog gene from *GDH2* occurred after the evolutionary bifurcation that separated bryophytes and tracheophytes. Experiments conducted on *Marchantia polymorpha* and *Calyptogeia fissa* grown in vitro and compared to *A. thaliana* demonstrated through in gel activity detection and monodimensional Western Blot that the aminating activity of GDH resulted in strongly enhanced responses to ammonium excess in liverworts as well, even if at a different extent compared to *Arabidopsis* and other vascular species. The comparative analysis by bi-dimensional Western Blot suggested that the regulation of the enzyme could be, at least partially, untied from the protein post-translational pattern. Finally, immuno-electron microscopy revealed that the GDH enzyme localizes at the sub-cellular level in both mitochondria and chloroplasts of parenchyma and is specifically associated to the endomembrane system in liverworts.

Alessandro Petraglia and Francesca Degola contributed equally to this work.

This is an open access article under the terms of the [Creative Commons Attribution](https://creativecommons.org/licenses/by/4.0/) License, which permits use, distribution and reproduction in any medium, provided the original work is properly cited.

© 2023 The Authors. *Physiologia Plantarum* published by John Wiley & Sons Ltd on behalf of Scandinavian Plant Physiology Society.

1 | INTRODUCTION

During decades, nitrogen-assimilating enzymes in plants have been extensively investigated under different points of view, producing a comprehensive literature on biochemical, genetic and functional aspects. Mainly conducted on few species at first, because of their economic and ecological importance (Galvez et al., 1999; Ireland & Lea, 1999; Lam et al., 1996; Mifflin & Lea, 1980; Temple et al., 1998), these explorations have also been gradually extended to other plants, such as the model species *Arabidopsis thaliana* and woody species. Being toxic to all living organisms, ammonium (NH_4^+) management is critical also in plants: in fact, since intracellular concentrations that exceed 1 mM usually result impairing all photosynthetic reactions within the chloroplast, it is essential that NH_4^+ is rapidly and effectively assimilated and converted into non-toxic forms. Glutamine and glutamate are compounds primarily synthesized for this purpose, but while glutamine is produced by glutamine synthetase (GS), both glutamine oxoglutarate aminotransferase (GOGAT; also known as glutamate synthase) and glutamate dehydrogenase (GDH; NAD(H)-GDH, EC 1.4.1.2) are responsible for glutamate biosynthesis (Figure 1). In contrast with the GS/GOGAT cycle, the GDH-dependent amination of 2-oxoglutarate does not consume energy, and, due to its ability to also function in the direction of glutamate biosynthesis when ammonium is abundant (Melo-Oliveira et al., 1996; Miyashita & Good, 2008), the GDH is thought to be the major NH_4^+ assimilatory enzyme when energy is limiting.

Being the precursor of other amino acids such as proline and arginine, glutamate is a central molecule in the metabolism in higher plants: it plays key roles not only as a metabolite, an energy-yielding substrate and a structural element in proteins, but also as a signaling molecule, an osmotic regulator for the organellar pH and is a pivotal character of plant autotrophy, being the precursor for chlorophyll synthesis in developing tissues (Yaronskaya et al., 2006). Consequently, many of the biochemical and molecular aspects involved in the enzymatic activities governing its metabolism are considered of major interest (Forde & Lea, 2007 and references therein). Amongst them, the role of GDH in glutamate management is one of the most controversial and has been repeatedly investigated and reviewed (Kwinta & Bielawski, 1998; Oaks & Hirel, 1985; Tercé-Laforgue et al., 2013; Tercé-Laforgue, Dubois, et al., 2004; Tercé-Laforgue, Mäck, et al., 2004).

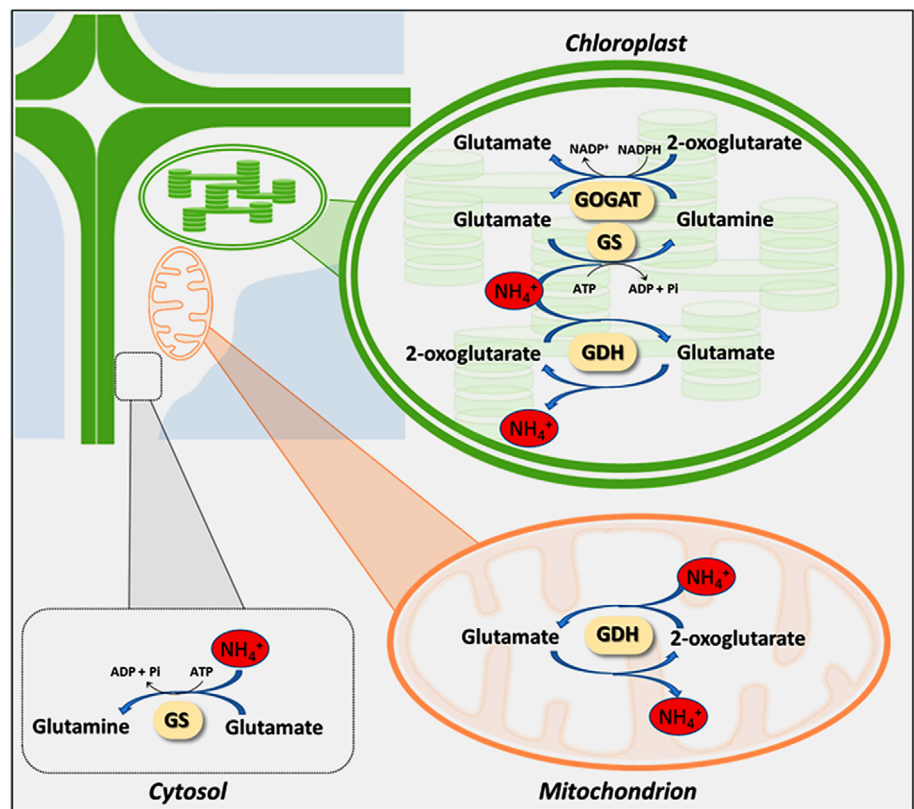
Present in bacteria as homohexamers, GDH enzymes have evolved into two families with different oligomeric structures in Eukaryotes: a tetrameric organization obtained by the association of ~115 kDa subunits has been found in fungi, while in vertebrates GDH is present in the only form of homohexamers (Britton et al., 1992). In plants, both homo- or heterohexamers exist and are composed by subunits of 43–50 kDa (Kwinta & Bielawski, 1998; Srivastava & Singh, 1987; Stewart et al., 1980). Although the structure, function and regulation of GDH is well established in bacteria, fungi and animals, its controversial role in the physiology of ammonium assimilation pathway in plants is still debated, and its structural and regulatory features are still object of investigations (Dubois

et al., 2003; Mifflin & Habash, 2002; Tercé-Laforgue et al., 2013). It has been demonstrated that in angiosperms at least two GDH genes encode two subunits (α and β) that randomly associate in α and β homo- or heterohexamers, giving origin to seven distinct GDH isoenzymes (Qiu et al., 2009; Thurman et al., 1965; Turano et al., 1997) whose relative abundance depends either on the organ or the physiological status of the plant (Lehmann et al., 2011; Restivo, 2004; Skopelitis et al., 2007; Turano et al., 1996; Watanabe et al., 2007). In *Arabidopsis* the α and β subunits that form the NADH-GDH isoenzymes are encoded by *GDH2* and *GDH1* genes, respectively, but a third gene, named *GDH3*, was found to code for an additional subunit termed γ . This subunit is actively transcribed in specific organs such as in the vasculature of root tissues and/or during specific developmental stages or under specific conditions (Fontaine et al., 2012; Igarashi et al., 2009; Yamada et al., 2003). At the same time, GDH of plants was found to share more similarities to the archaeobacterial homologous than to eukaryotic GDH, including the amino acid sequence and a significant thermostability (Pavesi, 2014; Pavesi et al., 2000; Syntichaki et al., 1996). Phylogenetic analysis conducted on the entire family of Glu/Leu/Phe/Val (ELFV) dehydrogenases, to which GDH belongs, revealed the existence of two distinct types in *Streptophyta*: the cluster which contains *AtGDH1* and *AtGDH3* as type I, and the cluster which contains *AtGDH2* as type II (Grzechowiak et al., 2020).

In plants, GDH isoenzymes have been generally assumed to be located in the mitochondrial matrix (Kwinta & Bielawski, 1998), where they are supposed to exert their major role for glutamate catabolism under carbon and N-limiting conditions (Tercé-Laforgue, Dubois, et al., 2004; Tercé-Laforgue, Mäck, et al., 2004), and only sporadically in the cytoplasm (Aubert et al., 2001; Stewart et al., 1995). However, a plastidial activity and expression of the protein have also been reported in soybean and *Chlamydomonas reinhardtii* (Bhadula & Shargool, 1991; Fischer & Klein, 1988). Detailed tissue analyses conducted on root, leaf and stem sections showed that in leaves the enzyme localizes mainly, if not exclusively, in the palisade parenchyma cells, while in stems and roots it has been described in phloem companion cells only (Fontaine et al., 2012; Tercé-Laforgue et al., 2013; Tercé-Laforgue, Dubois, et al., 2004; Tercé-Laforgue, Mäck, et al., 2004). But what might be the distribution of this enzyme at both, tissue and subcellular level, in plants that do not possess the same complexity of organs and vascular system of tracheophytes, is still to be acquired. Indeed, there is currently not enough information on the GDH structure and regulation in bryophytes.

Due to their unique physiology and ecology, bryophytes serve as ecosystem engineers, providing important ecological services including nitrogen and carbon fixation (Barger et al., 2016; Benalp, 2001; Oliveira & Maciel-Silva, 2022). It is quite clear that they differ from vascular species in influencing the cycling of elements and energy flow, but the metabolic strategies that make them such talented colonizers have been only partially explored (Degola et al., 2022). Amongst them, how bryophytes fix, transform, and manage carbon and nitrogen supposedly played a pivotal role. Ammonia-assimilating activity of GDH and GS/GOGAT enzymes has been reviewed for a small

FIGURE 1 Simplified scheme of ammonia assimilation in plants. It is governed in plants at chloroplast, mitochondria and cytosol level by the Glutamine Synthetase/Glutamate Synthase (GS-GOGAT) complex and the Glutamate Dehydrogenase (GDH).



selection of bryophyte species in 1979 (Lee & Stewart, 1979), but only in 1984 the correlation between this activity and the supply of nitrogen and other nutrients dependent on the environment was actually investigated, providing spectrophotometric evidence of GDH activity in eight mosses and four liverworts (Meade, 1984). In 1997, the glutamate dehydrogenase of *Sphagnum fallax* was partially characterized: its presence was determined in mitochondria but not in the chloroplast fraction, and its activity proved to be enhanced by the ammonium increase in the nutrient solution (Heeschen et al., 1997). Despite the fact that the preferred sources of inorganic N have been investigated in subtropical epiphytic bryophytes with an eye on ammonia-assimilating metabolism (Song et al., 2016), to our knowledge no significant attempts have been made to comprehensively characterize the functioning and the role of GDH in non-vascular land plants. Our effort in drawing a portrait of GDH enzyme in liverworts is addressed to provide a better understanding of the metabolism strategy of bryophytes to survival and adaptation, and aims at shedding light on some key features that could have contributed to their success in colonizing the most various environments during terrestrialization. We exploited various methodologies like sequence analysis, zymogram techniques, 1D and 2D Western Blotting, LC-MS targeted metabolomic analysis, and electron microscopy to examine and compare key characteristics of GDH in seven liverwort species, carefully selected from six distinct families across two orders of Marchantiophyta. The goal was to investigate: (i) the phylogenetic relationship between the GDH protein of liverworts and vascular plants; (ii) the number, composition and possible post-translational modification of GDH isoenzymes; (iii) their

sensitivity at thermal inactivation on a species- and organ-basis; (iv) the enzyme modulation in response to ammonium exposure, and (v) its localization at tissue and sub-cellular level.

2 | MATERIALS AND METHODS

2.1 | Plant material

Liverwort species used in this study were collected from natural populations in the Tuscan-Emilian Apennines (Parma, Italy). Three species of complex thalloid liverworts belonging to three different families within the order Marchantiales were chosen amongst Marchantiopsida (*Lunularia cruciata*: Lunulariaceae; *Marchantia polymorpha*: Marchantiaceae; *Conocephalum conicum*: Conocephalaceae) and five species belonging to three different families of the order Jungermanniales were chosen within Jungermanniopsida (*Pellia epiphylla*: Pelliaceae; *Plagiochila porelloides*: Plagiochilaceae; *Calyptogeia fissa*: Calypogeiaceae; *Radula complanata*; and *Frullania dilatata*: Porellales). Samples of approximately 5×5 cm from each population were collected, and three different populations were sampled for each species. The plant material was stored on their substrate for 3–4 days in a growth chamber at 25°C and 16/8 h light/dark photoperiod ($150 \mu\text{mol photons m}^{-2} \text{s}^{-1}$) before processing. For electrophoretic analyses, samples were washed under running water to remove soil and residues, then manually cleaned and separated from other species under a stereo microscope and washed in sterile bi-distilled water for

15 min with a magnetic stirrer. Finally, tissues were paper drained, instantly frozen in liquid nitrogen and stored at -80°C until processing. *Arabidopsis thaliana* L. (ecotype Columbia, Col-0) was also used as a reference species.

2.2 | Axenic cultures and growth conditions

Axenic cultures of *M. polymorpha*, *L. cruciata*, and *C. fissa* were obtained from surface-sterilized gemmae: they were manually recovered from cups of *M. polymorpha* and *L. cruciata*, then sterilized for 5 min in a 0.2% (v/v) sodium hypochlorite solution (commercial 5% sodium hypochlorite, 0.1% (v/v) Tween[®]20). Gemmae were rinsed four times in sterile bi-distilled water and seeded in Petri dishes with Bryophyte Medium (BM; Baslerova & Dvorakova, 1962) modified as follows: NH_4NO_3 80 g l^{-1} , KH_2PO_4 136 g l^{-1} , $\text{MgSO}_4 \cdot 7\text{H}_2\text{O}$ 120 g l^{-1} , $\text{CaCl}_2 \cdot 2\text{H}_2\text{O}$ 110 g l^{-1} , $\text{FeCl}_3 \cdot 6\text{H}_2\text{O}$ 16.2 g l^{-1} , agar 0.8% (w/v), and 0.2% (w/v) sucrose. Cultures were grown for 7 days at 25°C with a 16/8 h photoperiod (150 $\mu\text{mol photons m}^{-2} \text{s}^{-1}$), then transferred to half-strength Murashige–Skoog agar complete medium (MS; #M0222, Duchefa) containing 2% (w/v) sucrose and 0.8% (w/v) agar and maintained at 25°C with a 16/8 h photoperiod (150 $\mu\text{mol photons m}^{-2} \text{s}^{-1}$). Gemmae of *C. fissa* were recovered by vortexing branches in a water solution, separated by centrifugation, surface-sterilized and propagated as for *M. polymorpha* and *L. cruciata*. Due to the presence of algal endophytes, *C. fissa* axenic cultures were subjected to serial transfers of clean cuttings from mature branches in half-strength MS medium, until the complete removal of contamination.

Once the axenic cultures were obtained, gemmae from reproductive structures were manually recovered and seeded in half-strength NH_4NO_3 -free MS medium (#M0238.0010, Duchefa), 1% (w/v) sucrose and 0.8% (w/v) agar, either amended with 5 mM NH_4^+ or not (supplied as 1 mM $(\text{NH}_4)_2\text{SO}_4$ plus 3 mM NH_4Cl); NO_3^- was added in form of 0.1 mM KNO_3 in the control medium ($-\text{NH}_4^+$). Cultures were maintained at 25°C with a 16/8 h photoperiod (150 $\mu\text{mol photons m}^{-2} \text{s}^{-1}$).

Arabidopsis axenic material was obtained by surface sterilizing seeds for 20 min with the diluted sodium hypochlorite solution previously described. The seeds were then washed three times with sterile bi-distilled water and stratified in half-strength MS amended with NH_4^+ or without it for two days in the dark at 4°C before incubating the plates at 25°C (16/8 h light/dark photoperiod, 150 $\mu\text{mol photons m}^{-2} \text{s}^{-1}$).

Plantlets were harvested after the desired time, weighed, frozen in liquid nitrogen and stored at -80°C . Three biological replicates were used for each species, and experiments were conducted in triplicates.

2.3 | Native proteins extraction and in gel GDH activity staining

Proteins were extracted from different plant tissues. About 200 mg of fresh weight tissue were homogenized in 200 μl of extraction

buffer [100 mM Tricine (pH 8.0), 10 mM MgSO_4 , 0.2% (v/v) β -mercaptoethanol, 0.5 mM PMSF, 40 mM CaCl_2 , 0.5% (w/v) polyvinylpyrrolidone, 1 mM EDTA and 0.05% (v/v) Triton X-100] in a 1.5 ml Eppendorf tube using a micropestle. After two rounds of centrifugation at 15 000g for 20 min at 4°C , the resulting supernatant was used for NAD-dependent, GDH in gel activity detection. Zymograms were performed as described by Loulakakis and Roubelakis-Angelakis (Loulakakis & Roubelakis-Angelakis, 1990), with minor modifications: the GDH activity staining solution (100 mM TrisHCl (pH 8.8), 53 mM sodium glutamate, 0.7 mM NAD, 0.03 mM phenazine methosulphate and 0.3 mM nitro blue tetrazolium) was supplemented with 0.4% (w/v) agarose and poured onto the gel. Enzyme activity staining was performed at 37°C in the dark and stopped by replacing the staining overlay with 5% (v/v) acetic acid solution. Protein concentration was determined according to Bradford (1976) with bovine serum albumin as standard. Equal amounts of 20 μg total proteins were loaded in each lane. For the thermal stability assessment of GDH isoenzymes, protein extracts were incubated at 65 or 80°C for 20 min, then chilled on ice for 1 min, briefly centrifuged to pellet possible protein aggregates and then loaded on the native gel. Zymograms were performed on three independent plant samples, and experiments were performed in triplicates. A densitometric analysis was conducted on acquired gel images by using the QuantityOne[®] Software (BioRad). For thermal inactivation assays, protein native extracts were treated at 65 and 80°C for 20 min, then, subjected to native-PAGE followed by NAD-GDH in gel staining. Not treated extracts were used as a control.

2.4 | Mono- and two-dimensional Western Blot characterization of GDH proteins

Total proteins from 200 mg of fresh weight plant tissues were extracted with 400 μl lysis buffer (50 mM TRIS-HCl pH 7.5, 2 M thio-urea, 7 M urea, 2% (v/v) Triton X-100, 1% dithiothreitol (DTT), 2% (w/v) polyvinylpyrrolidone (PVPP), 1 mM phenylmethylsulphonyl fluoride (PMSF), and 0.2% (v/v) β -mercaptoethanol). Protein concentration was determined according to Bradford (1976).

For mono-dimensional electrophoresis, 15 μg of total proteins per well were loaded on a 12% SDS-polyacrylamide gel, run at 200 V for 45 min, and electro-transferred at 100 V for 60 min onto a nitrocellulose membrane (GE Healthcare Bio-Sciences AB) using the Mini Trans-Blot cell apparatus (Bio-Rad Laboratories). For two-dimensional electrophoresis, protein extracts were precipitated with trichloroacetic acid/acetone, then re-suspended in a rehydration buffer (8 M urea, 2% w/v CHAPS, 50 mM DTT, 0.2% v/v Bio-Lyte 3/10 Bio-Rad ampholytes, Bromophenol Blue in traces), and 125 μg of total proteins were loaded on 7 cm-long ReadyStrip[®]IPG Strips, pH interval 3.0–10.0 (Bio-Rad Laboratories). 2D-electrophoresis was carried out using the Protean IEF system (Bio-Rad Laboratories), following the manufacturer's instruction. Gels were then stained with SYPRO[®] Ruby Protein Stain (Bio-Rad Laboratories) and images acquired using the VersaDoc Imaging System (Bio-Rad Laboratories).

After the image digitization, gels were immersed for 20 min in running buffer and briefly washed with the electro-blot transfer buffer (25 mM Tris, 192 mM glycine, pH 8.3, 20% (v/v) methanol), then proteins were electro-transferred on a nitrocellulose membrane as described above. For both 1D- and 2D-Western Blot analyses, protein loading and transfer efficiency were verified by the Ponceau-S staining. Immunoreactivity was assayed with an antiserum raised against the GDH of *Vitis vinifera* L. (Loulakakis & Roubelakis-Angelakis, 1991), diluted 1:2000 in 5% (w/v) skim milk blocking buffer and probed at RT for 1 h 30 min. Peroxidase activity of anti-rabbit secondary antibody was developed by ECL solutions (GE Healthcare Western Blotting Detection Amersham™ ECL Prime, Fisher Scientific Italia), following the manufacturer instructions. A densitometric analysis was conducted on acquired gel images by using the QuantityOne® Software (BioRad). Analyses were performed in triplicates on three independent plant samples, and experiments were performed in triplicates.

2.5 | Sequence retrieval and analysis

Amino acid sequences of two vascular and seven liverwort species were retrieved from the publicly available databases NCBI (Arabidopsis: NP_197318.1, NP_001119183.1, AT3G03910.1; *Nicotiana plumbaginifolia*: O04937, Q9LEC8; *M. polymorpha*: A0A2R6XCJ8, A0A176VW80) and CNSA (*L. cruciata*: scaffold-TXVB-2013247, scaffold-TXVB-2013248; *M. polymorpha*: scaffold-JPYU-2039183; *Pellia* sp: scaffold-PIUF-2087126; *Radula lindenbergiana*: scaffold-BNCU-2014111, scaffold-BNCU-2014112, scaffold-BNCU-2014113; *C. conicum*: scaffold-ILBQ-2006143; *C. fissa*: scaffold-RTMU-2183279; *Frullania* sp: scaffold-TGKW-2139530). Sequence multiple alignment and identity matrix have been obtained with the BioEdit Software version 7.2.5 (Hall, 1999). The CUPSAT (Cologne University Protein Stability Analysis Tool) web-server was used to estimate changes in protein stability upon amino acid substitution, that gives the stability prediction upon mutation for all the amino acid mutations for a specific position: the online tool assesses the amino acid environment around the substituted position; secondary structure specificity and solvent accessibility are also used to determine the amino acid environment. Amino acid atom potentials of 40 amino acid atoms from Melo-Feytmans were used to construct the radial pair distribution function (Parthiban et al., 2006; Parthiban, Gromiha, Abhinandan, et al., 2007; Parthiban, Gromiha, Hoppe, et al., 2007). Evolutionary relationships were inferred by aligning sequences from each of Embryophyta groups (mosses, hornworts, liverworts lycophytes, ferns, gymnosperms, dicots, and monocots): sequences were retrieved by blasting the *N. plumbaginifolia* amino acid sequence against “The 1,000 Plants Project” Database on the China National Gene Bank (<https://db.cngb.org/blast/>), records with high scores and with a length of 411 amino acids were kept and blasted against the NCBI nr database to confirm the presence of conserved domains (File S1). Sequences were aligned with MAFFT (File S2) using the European Bioinformatics Institute server ([https://](https://www.ebi.ac.uk/Tools/msa/mafft/)

www.ebi.ac.uk/Tools/msa/mafft/), the resulting alignment submitted to the IQ-Tree using the CIBIV server (<http://iqtree.cibiv.univie.ac.at/>), and results finally were visualized in MEGA XI (Kumar et al., 2018). GDH amino acid sequence from *Homo sapiens* was used as outgroup.

2.6 | Amino acid content determination

2.6.1 | Plant material

Plantlets of *M. polymorpha* and *C. fissa* were sown and maintained in MS-NH₄NO₃ either amended or not with 5 mM NH₄⁺, and were collected after 30 days of growth. Six young, fully developed and green lobes from as many gametophytes per Petri dish were collected and pooled, discarding rhizoids, for a total of three independent biological replicates. Growth medium residues were eliminated by washing the plant tissues with 5 ml MilliQ water into 15 ml tubes, vortexing 10 s, and rinsing with fresh MilliQ water, then the samples were dried onto a Whatman® filter paper, frozen in liquid nitrogen, and stored at −80°C.

2.6.2 | Amino acid extraction

The extraction protocol was performed as previously described (Guo et al., 2013; Pan et al., 2014) with slight modifications. The plant frozen material was homogenized in liquid nitrogen, weighed to 70 mg and extracted in 10 volumes (w/v) of LC-MS grade water (Honeywell, Riedel-de Haën). Samples were vortexed for 30 s and centrifuged at 13 000g at 4°C for 15 min. The supernatant was collected and diluted 1:10 with LC-MS grade water (Honeywell, Riedel-de Haën) for the analysis of almost all protein amino acids, or 1:50 for the analysis of glutamic acid and arginine specifically. The diluted extracts were filtered with 0.2 µm pores Minisart RC4 filters (Sartorius) prior to the LC-MS analysis.

LC-MS conditions for targeted metabolomics analysis: Targeted metabolomics analysis was carried out as previously described by Wen et al. (2019) with modifications. Samples were kept at 8°C in the autosampler and 0.5 µl were randomly injected to an ACQUITY I CLASS UPLC system (Waters), equipped with an ACQUITY UPLC BEH amide column (2.1 mm × 100 mm, 1.7 µm; Waters) and a guard column BEH amide Vanguard Pre-column (2.1 mm × 5 mm, 1.7 µm; Waters) maintained at 25°C. Solvents used for the chromatographic gradient were: (A) 0.2% formic acid (Biosolve Chimie) in water (Honeywell) and (B) 0.2% formic acid in acetonitrile (Honeywell). The gradient was set as followed: 90–74% B in 4.5 min, 74–55% B in 1 min, isocratic condition (55% B) for 1 min and return to initial condition in 0.1 min. Subsequently, the system was equilibrated in 90% B for 8.4 min. Total analysis time was 15 min. The flow rate was set at 0.3 mL min^{−1}. Purge solvent was water:acetonitrile 20:80 (v/v) and wash needle solvent water:acetonitrile 80:20 (v/v). The column was directly connected to a PDA and a Xevo G2-XS qTOF mass

spectrometer (Waters), equipped with an electrospray ionization (ESI) source, operating in either positive or negative ionization modes, and controlled by MassLynx v4.1. The ion source conditions were as follows: capillary voltage 3 kV, sampling cone voltage 10 V, source offset voltage 30 V, source temperature 110°C, desolvation temperature 450°C, cone gas flow rate 30 l h⁻¹, and desolvation gas flow rate 800 l h⁻¹. Argon was used to induce collision-induced dissociation. A multiple reaction monitoring (MRM) method was created to acquire data in sensitivity and continuum mode, with a scan range from 20 to 250 Da and scan time of 0.05 s. Amino acid ion precursors were used as quantifiers and level comparison was performed by using the corresponding peak areas, whereas the ion products (fragments) were used as qualifiers to confirm metabolite identity (Table S1). Accuracy of the mass spectrometer was confirmed by injecting a solution of 100 µg µl⁻¹ leucine enkephalin (waters) with a flow rate of 10 µl min⁻¹, that was fragmented to generate signals of 120.0813 m z⁻¹ in positive mode and 236.1035 m z⁻¹ in negative mode. Amino acid identification was performed by comparing the m/z values of molecular and daughter ions, and the retention times against a mixture including all the amino acids at authentic commercial standards (Sigma Aldrich; Guo et al., 2013; Pan et al., 2014).

2.7 | In planta GDH activity detection

NAD-GDH activity was assessed directly in plant tissues through a specific histochemical in planta assay, according to Marchi et al. (2021): fresh thalli of *M. polymorpha* were harvested from 30 days-old cultures grown on complete, half-strength MS, washed with sterile demineralized water, gently dried on sterile filter paper and, prior to the staining step, exposed at 70°C for 15 min to inactivate non-specific enzymes. After thermal inactivation, tissues were placed into 1.5 ml tubes, dipped in 1 ml of staining solution (100 mM Tris-HCl (pH 8.8), 53 mM Na-glutamate, 0.7 mM NAD, 0.03 mM phenazine methosulfate and 0.3 mM Nitro Blue Tetrazolium (NBT)), subjected to vacuum infiltration for 10 min and then incubated at 37°C until color development. Samples dipped in a staining solution without sodium glutamate were used as control for the reaction specificity. Destaining of treated samples was not necessary before acquiring images with a stereo microscope. Observations were conducted on three biological replicates, and the assay was conducted in triplicates.

2.8 | Immunolocalization of GDH enzymes in thalli of *M. polymorpha*

2.8.1 | Sample preparation

Fifteen randomly chosen thallus segments were excised from 30 days-old cultures grown on complete, half-strength MS. Segments were cut into small portions of 6–7 mm in length, fixed in 0.2% glutaraldehyde, rinsed in 0.1 M phosphate buffer, pH 7.4, and dehydrated

in graded EtOH series (25, 50, 75%, 30 min for each step) at 4°C. After 1 h of the final 100% EtOH step, the samples were infiltrated for 30 min in a hard-grade London Resin White: 100% ethanol mixture (LRW; Electron Microscopy Sciences) in the proportion 1:2, followed by 30 min in 2:1 LRW:ethanol, and 100% LRW overnight at room temperature. A replacement with fresh mixture was applied after 1 h from the beginning of the infiltration step. Samples were embedded in 1.5 ml tubes using fresh LRW containing benzoyl peroxide 2% (w/w), according to manufacturer's instructions, and polymerized for 24 h at 60°C (Musetti et al., 2002).

2.8.2 | Immunogold-labeling and transmission electron microscopy observation

To visualize the presence and distribution of GDH in LR-White-embedded plant tissues, the immunogold-labeling technique was performed. Several serial ultrathin sections (60–70 nm) of three LR-White-embedded samples from each plant were cut using an ultramicrotome (Reichert Leica Ultracut E ultramicrotome, Leica Microsystems) and collected on carbon/formvar coated 400 mesh nickel grids (Electron Microscopy Sciences). Unspecific binding sites were blocked by placing grids carrying the sections on droplets of blocking solution containing 5% normal goat serum (NGS) diluted in TBS, pH 7.6, for 1 h at RT. Grids were then incubated for 6 h at room temperature the antiserum against GDH diluted 1:70 in blocking solution, the same used for Western Blot analyses. All grids were then rinsed five times with TBS and treated for 2 h at room temperature with secondary goat anti-rabbit antibody coated with 10 nm colloidal gold particles, diluted 1:50 in TBS (GAR 10; Auro Probe EM GAR G10 Amersham). Sections were stained with UAR-EMS (uranyl-acetate replacement stain, Electron Microscopy Sciences), then observed under a Philips CM 10 TEM (FEI) operating at 100 kV. Ten non-serial cross-sections from each sample were observed under a PHILIPS CM 10 (FEI) TEM, operated at 80 kV and equipped with a Megaview G3 CCD camera (EMSIS GmbH). For the immunogold-labeling assay, negative controls were represented by sections incubated with the secondary antibody alone, that is, avoiding the primary antibody incubation step.

2.9 | Statistical analysis

Enzyme activity results from densitometric data and amino acid relative abundance results obtained with LC-MS were checked for normality and subjected to statistical analysis with the “IBM SPSS Statistics 24” software. One-way ANOVA with Dunnett's post-hoc test and Student's *t*-test were applied to determine significant differences between treated and untreated cultures in NH₄⁺ supplementation experiments (*p* < 0.05 for densitometric data, *p* < 0.05 and *p* < 0.01 for amino acid analysis). Data are presented as means ± SD of biological replicates (*n* = 3 independent pools of plant material).

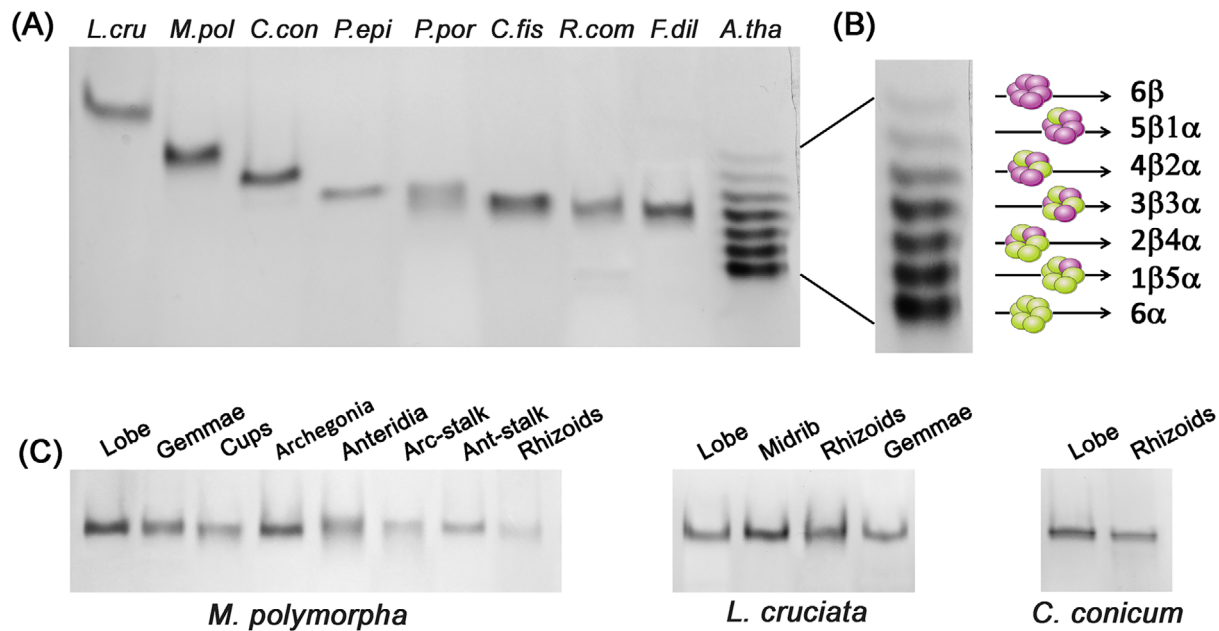


FIGURE 2 GDH isoenzyme patterns of the selected Liverwort species, *L. cruciata*, *M. polymorpha*, *C. conicum*, *P. epiphylla*, *P. porelloides*, *C. fissa*, *R. complanata* and *F. dilatata*, compared with the *Arabidopsis* GDH profile. Zymogram of NAD-GDH was obtained for the gametophytes of all species (A) and compared with the isoenzyme pattern of *Arabidopsis* leaves (B). A native-PAGE was conducted on different organs of *L. cruciata*, *M. polymorpha*, and *C. conicum* (C): lobes, gemmae, cups, archegoniophores (archegonia and stalk), antheridiophores (antheridia and stalk), and rhizoids were extracted and analyzed separately. Analyses were performed on extracts from three independent pools of plant material.

3 | RESULTS

3.1 | The GDH enzyme in selected liverwort species revealed a single-banded, tissue non-dependent isoenzyme pattern, and a species-specific post-translational modification profile

A native-polyacrylamide gel electrophoresis (native-PAGE) was conducted on protein extracts from plant material collected in the natural environment to reveal the distribution of GDH isoenzymes in form of a zymogram. At first, extracts from whole gametophytes of *L. cruciata*, *M. polymorpha*, *C. conicum*, *P. epiphylla*, *P. porelloides*, *C. fissa*, *R. complanata*, and *F. dilatata* were analyzed. When compared with leaf extracts of *Arabidopsis thaliana* (Figure 2A), that consistently showed the presence of two 6α and 6β homohexamers and five α/β heterohexamers in a seven-banded profile (Figure 2B), the liverworts displayed a less complex electrophoretic profile: a single stained band was detected in almost all species, with the exception of *P. porelloides* that showed two separate signals (Figure 2B). The GDH profiles significantly differed amongst the liverwort species in terms of positioning; however, with the only exception of *L. cruciata*, whose GDH isoenzyme is located above the most cathodic isoform of *Arabidopsis* (corresponding to 6β homohexamer). In all the species analyzed, the position of GDH signal fell between its first and fourth band (corresponding to 5β1α heterohexamer). No signals were detected in the anodic half of the electrophoretic profile.

Then, a finer dissection of tissue-specific NAD-GDH activity was tentatively pursued, following the hypothesis that, as already demonstrated for some angiosperms, different isoforms of the enzyme might

be differently expressed in different organs. Diverse organs from the thallose species *L. cruciata* (lobes, midrib, gemmae, and rhizoids), *M. polymorpha* (lobes, gemmae, cups, archegoniophores split in archegonia and stalk, antheridiophores split in antheridia and stalk, and rhizoids) and *C. conicum* (lobes and rhizoids) were separately extracted and analyzed (Figure 2C). No differences were found in the isoenzyme patterns on a tissue/organ basis, as the electrophoretic profiles, shown by dissected tissues, perfectly matched with those obtained for lobes in all the three species.

As zymography yields quantitative and qualitative information of an enzyme but it is unable to separate two or more isoenzymes that share highly similar physicochemical properties, such as different phosphorylation patterns, an immunochemical approach was exploited by using a GDH-antiserum raised against the GDH of *Vitis vinifera* L. (Loulakakis & Roubelakis-Angelakis, 1990, 1991). As shown in Figure 3A, the presence of an immunoreactive signal has been confirmed in all samples: a single band of ~45 kDa compatible with *Arabidopsis* GDH subunits was detected, that showed very poorly noticeable differences in molecular weight amongst the liverwort species. In terms of relative abundance, the bryophyte extracts revealed a level of GDH protein lower than what obtained in *Arabidopsis*, with the exception of the *M. polymorpha* gametophyte whose signal appeared more intense than in other liverworts.

When plant extracts were subjected to 2D-WB analysis, different signal patterns were produced. All samples showed a single cluster localized at an apparent molecular weight of ~45 kDa, restricted to an apparent isoelectric point range between 5.2 and 7.5, but they varied in the number of total spots and their relative intensity

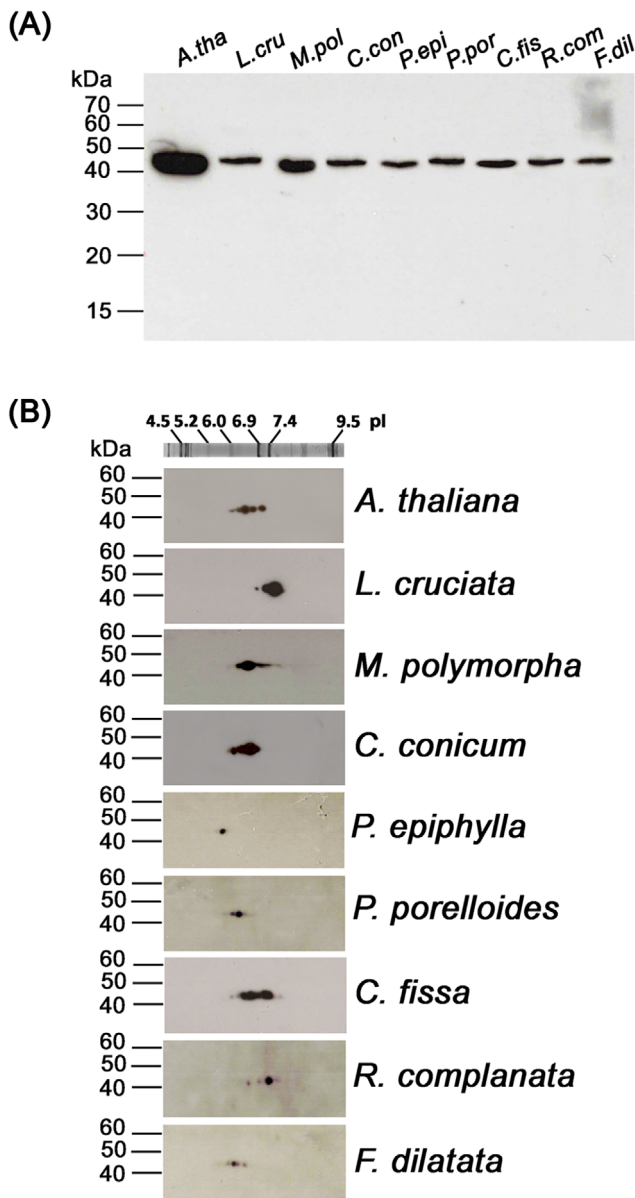


FIGURE 3 Immunochemical characterization of GDH through Western blot. Immunochemical characterization of GDH in *L. cruciata*, *M. polymorpha*, *C. conicum*, *P. epiphylla*, *P. porelloides*, *C. fissa*, *R. complanata*, and *F. dilatata* gametophyte, obtained with 1D-(A) and 2D-(B) Western Blot. Total protein extracts from liverwort species collected in natural environments are compared with Arabidopsis leaf extracts (*A. th.*; GDH molecular weight = 44.5 kDa) as a reference. An antiserum raised against GDH of *V. vinifera* was employed. Same amount of total proteins have been loaded. An IEF marker was used to outline the pI of GDH isoforms detected (B; upper row). Analyses were performed on extracts from three independent pools of plant material.

(Figure 3B). When compared to the Arabidopsis pattern, which displayed three major spots of five in total, the liverwort's profile showed one main spot at most, independently of the total number detected. A unique exception was represented by *C. fissa*, whose profile seemed more similar to Arabidopsis than the other species analyzed.

The presence of diverse GDH-immunoreactive clusters clearly indicated that the protein is subjected to different post-translational modifications in the different species, as the separation by isoelectrofocusing prior 2D-WB enables the individual detection of alternative protein species with the same specific antibody (Herzog et al., 2020). Notably, the 2D-WB pattern of *P. epiphylla* was found to be the only one to display a single detectable isoform, suggesting for this Metzgeriales' representative a post-translational modification profile less complex than the other species examined.

As the contribution of phosphoryl groups to a peptide molecular weight accounts for ≈ 1 kDa/single group and due to the resolution limit of standard SDS-PAGE, phosphorylation was assumed the most probable post-translational modification of GDH detected in this 2D-WB analysis.

3.2 | GDH enzyme is less thermoresistant in liverworts than in Arabidopsis, but a tissue-specific response to temperature inactivation has been detected in *M. polymorpha*

One of the main distinctive features of GDH, is the great stability the enzyme retains during the exposure to high temperatures (Ohshima & Nishida, 1993; Syntichaki et al., 1996). Here it has been investigated in liverworts through a thermal inactivation assay. Zymograms obtained from plant material collected in natural environments were compared to the GDH profile of Arabidopsis (Figure 4). The 6α and 6β homohexamers as well as α/β heterohexamers readily visible in Arabidopsis leaf extracts, did not exhibit any change in terms of signal intensity even after exposure to the highest temperature (Figure 4A), as expected. On the contrary, the enzyme showed a different behavior in liverwort extracts: *L. cruciata* GDH proved to be the most sensitive to temperature increase amongst Marchantiales, as at 80°C the signal corresponding to the GDH activity completely disappeared. The same sensitivity was also observed in both Porellales (*F. dilatata* and *R. complanata*), while the less thermoresistant species *C. fissa* showed a GDH activity dramatically impaired at 65°C already. Intriguingly, the thermal treatment caused an alteration of the electrophoretic behavior of the enzyme: the temperature increase determined a more cathodic positioning of GDH signal in *M. polymorpha* and *C. conicum*, and a more anodic shift in *P. porelloides* (Figure 4A). The same alteration in electrophoretic positioning of the GDH signal has been also observed when a comparative analysis of the enzymes thermostability in different organs was conducted on *M. polymorpha*, even though few tissue-specific differences occurred (Figure 4B). After 80°C exposure, extracts obtained from both lobes and cups replicated the shift toward the cathode showed by the whole sporophyte extract, as well as extracts from archegonia and antheridia at a lighter extent (Figure 4B). On the contrary, the zymogram of archegoniophore and antheridiophore stalks did not display any temperature-dependent change, neither in terms of GDH signal positioning nor in terms of enzyme activity, as observed for the other organs and in the case of Arabidopsis root extracts.

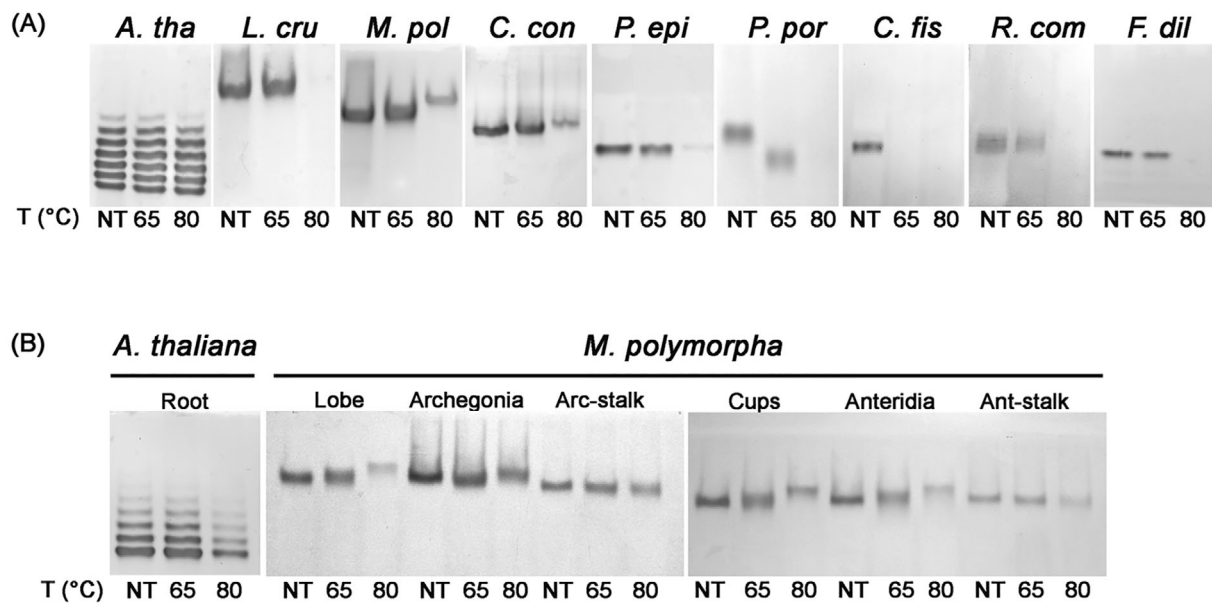


FIGURE 4 Thermal stability of GDH isoenzymes. Native protein extracts of liverworts and Arabidopsis were incubated for 20 min at increasing temperature (from 65 to 80°C) and subjected to native PAGE followed by NAD-GDH in gel activity staining. Untreated extracts were loaded as control (not treated, NT). Gametophyte extracts from all the selected species were compared with an Arabidopsis leaf extract (A). Different organs from *M. polymorpha* (lobes, cups, archegoniophore's archegonia and stalk, antheridiophore's antheridia and stalk) were extracted, treated and analyzed separately, and compared with an Arabidopsis root extract (B). Analyses were performed on extracts from three independent pools of plant material.

3.3 | Liverwort's GDH is sister to the monophyletic clade of GDH2 and GDH1/3, and showed a high similarity to Arabidopsis GDH2

Amino acid sequences were retrieved from Embryophytes groups (mosses, hornworts, liverworts, lycopphytes, pteridophytes, gymnosperms, dicots, and monocots) and aligned to explore the phylogenetic relationships amongst GDH proteins of liverworts and tracheophytes. The results of our analysis supported three separated clades for liverworts, mosses and hornworts (Figure 5). As well, a clear separation between Marchantiopsidae (*L. cruciata*, *M. polymorpha*, and *C. conicum*) and Jungermanniopsidae (*Pellia* sp., *C. fissa*, *R. lindenbergiana*, and *Frullania* sp.) was observed. Phylogenetically, the liverworts clade resulted in a sister group to angiosperms, that showed two main clades: one formed by amino acid sequences of GDH α subunit, that included *N. plumbaginifolia* GDHA and *A. thaliana* GDH2, and one formed by amino acid sequences of GDH β subunit (that included *N. plumbaginifolia* GDHB and *A. thaliana* GDH1 and GDH3). This suggests that a common ancestor possessing same properties of both modern GDH α and β isoenzymes has shared by liverworts and angiosperms, that has undergone a gene duplication in the latter. When the liverworts GDH protein sequences were compared to those from Arabidopsis, a slightly higher level of sequence conservation was found with respect to GDH2 (α subunit) rather than GDH1 (β subunit) in almost all the species considered. According to the sequence identity matrix, *L. cruciata* GDH protein showed 77.3% identity with GDH2 and

76.6% with GDH1, *C. conicum* 79% versus 78%, *Pellia* sp. 75.1% versus 74.4%, *C. fissa* 74.6% versus 73.9%, *R. lindenbergiana* 75.4% versus 74.2%, and *Frullania* sp. 74.2% versus 73.7%. On the contrary, *M. polymorpha* showed 77.6% identity with GDH2 but 78.5% with GDH1 (Table 1).

The multiple alignment performed on the amino acid sequences (Figure S1) was also exploited to carry out an analysis of the GDH protein C-terminus, which contains the Domain I (residues 1–181 and 333–411). This domain is located at the core of the D3-symmetric hexamer and is considered the key to the formation of the hexameric quaternary structure of GDH enzyme (Lesk, 1995). Three residues located in the 390–411 amino acid consensus sequence, namely 397, 406, and 411, were investigated in particular, being responsible for the low thermal stability of GDH3 in *A. thaliana* and *A. lyrata* (Marchi et al., 2014). A logo's graphical representation of the alignment of all the 17 sequences (Figure 6A) was compared with logos obtained from the alignment of GDH sequences of the two vascular species (Figure 6B), of all the six liverwort species (Figure 6C), of the thallose species (*L. cruciata*, *M. polymorpha*, and *C. conicum*; Figure 6D) and of the leafy species (*C. fissa*, *R. lindenbergiana*, and *Frullania* sp.; Figure 6E). All GDH sequences, except for Arabidopsis GDH3, showed V397 in substitution of I397, as well as L406 was found instead of I406. Interesting differences were observed for residues 398 and 391: N398, that is conserved in Arabidopsis, *N. plumbaginifolia* and other 15 species (Marchi et al., 2014), is substituted by G398 in liverworts. G391 that is shared by vascular

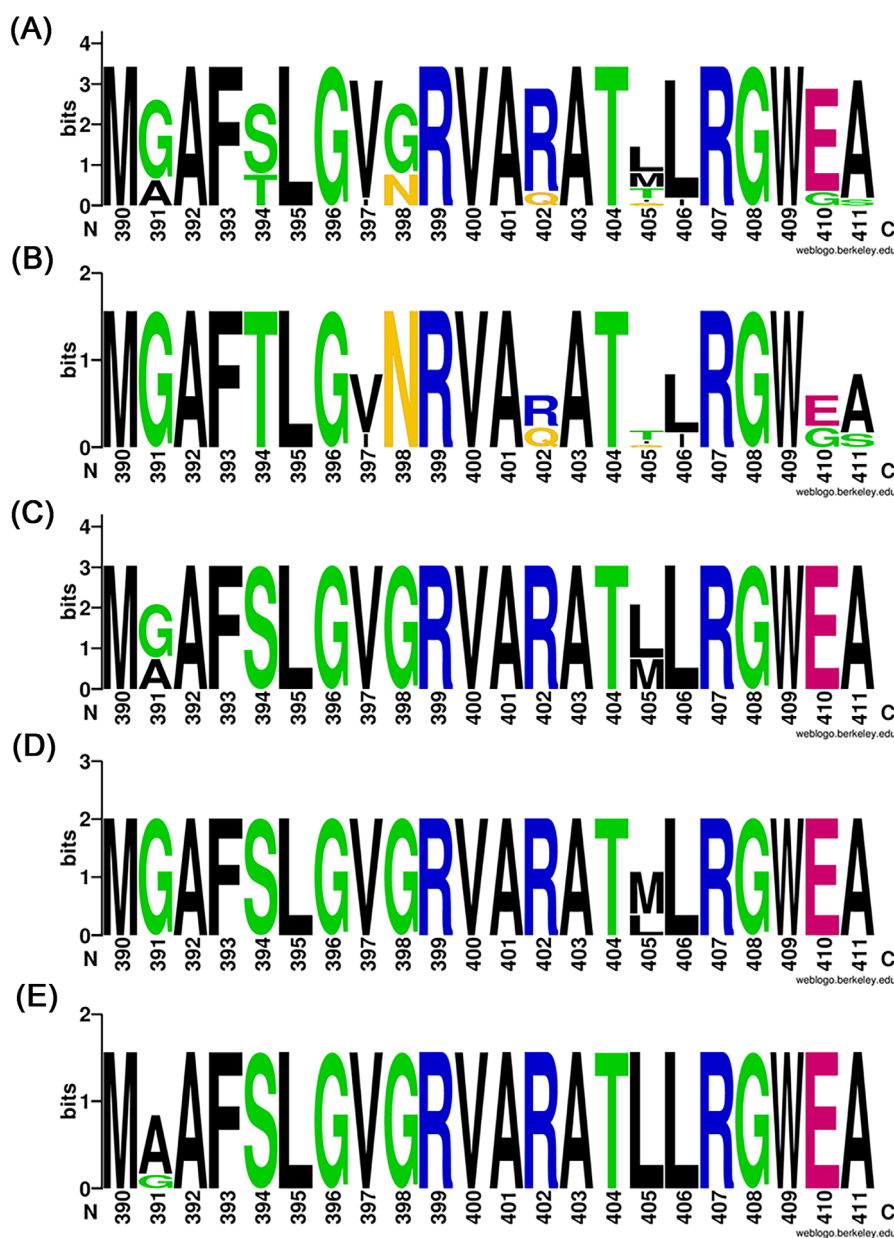


FIGURE 5 Phylogenetic tree obtained by aligning GDH amino acid sequences from Embryophytes (liverworts, mosses, hornworts, lycophytes, pteridophytes, gymnosperms, dicots, and monocots). Sequences well clustered according to each Embryophyte group. GDH from Marchantiopsidae and Jungermanniopsidae grouped separately within the liverworts clade, while Angiosperms displayed two main clades, one formed by amino acid sequences of GDH α subunit and one formed by amino acid sequences of GDH β subunit.

TABLE 1 Sequence identity matrix showing the sequence identity on 0–1 scale amongst GDH protein sequences; highest values in the GDH1/GDH2 comparison are gray-shaded.

	GDH1_A.th	GDH2_A.th	<i>L.cru</i>	<i>M.pol</i>	<i>C.con</i>	<i>Pellia_sp.</i>	<i>C.fissa</i>	<i>R.lind</i>	<i>Frull_sp.</i>
GDH1_A.th	1	0.805	0.766	0.785	0.781	0.744	0.739	0.742	0.737
GDH2_A.th		1	0.773	0.776	0.790	0.751	0.746	0.754	0.742
<i>L.cru</i>			1	0.922	0.905	0.878	0.827	0.824	0.819
<i>M.pol</i>				1	0.924	0.863	0.834	0.829	0.815
<i>C.con</i>					1	0.858	0.836	0.836	0.817
<i>Pellia_sp.</i>						1	0.836	0.849	0.834
<i>C.fissa</i>							1	0.832	0.812
<i>R.lind</i>								1	0.861
<i>Frullania_sp.</i>									1

FIGURE 6 LogoPlot of protein alignment of the GDH C-terminus from amino acid position 390–411 in selected species. A multiple alignment of 17 GDH sequences from two vascular plants (*Arabidopsis* and *N. plumbaginifolia*) and seven liverwort species (*L. cruciata*, *M. polymorpha*, *C. conicum*, *Pellia* sp., *C. fissa*, *R. lindenbergiana*, and *Frullania* sp.) was used to generate the sequence logo. Heights of letters indicate degree of conservation in units of maximum entropy expressed in bits. Colors indicate amino-acid similarity: KRH, blue; NQ, yellow; GST, green; DE, magenta; and AVLIPWFM, black. Logo from the complete alignment (A) was dissected in the logo representation of GDH from vascular species (B) and liverwort species (C). The latter has been further dissected in logo representation of GDH sequences from thallose (D) and leafy species (E). The bit score indicates the residue content for each position in the sequence. Logos were created with the Weblogo online tool (<https://weblogo.berkeley.edu>). The actual alignment is provided in Figure S1.



species, thallose liverworts, and *C. fissa*, is substituted by Alanine in the two *Porellales*. The possible effect of these substitutions on the protein stability was investigated with the CUPSAT prediction tool. According to the distortion model applied to Arabidopsis glutamate dehydrogenase isoform 1 (PDB Entry: 6YEI; PDB DOI: [10.2210/pdb6YEI/pdb](https://doi.org/10.2210/pdb6YEI/pdb)), the N398G substitution in particular was found to determine a de-stabilization of the protein structure under thermal denaturation (<http://cupsat.tu-bs.de/>. Accessed January 27, 2023).

3.4 | GDH aminating activity, protein expression, and isoenzyme patterns are differently responsive to NH_4^+ in *L. cruciata*, *M. polymorpha*, and *C. fissa*

In vitro cultures of *L. cruciata*, *M. polymorpha*, and *C. fissa* were exploited to characterize the GDH activity, thermal stability, protein abundance and post-translational pattern in response to ammonium. As experiments conducted on vascular plants like Arabidopsis, *Nicotiana tabacum*, *Medicago truncatula*, *V. vinifera* for investigating the non-redundant role of GDH in inorganic nitrogen assimilation typically used concentrations of exogenous NH_4^+ ranging from 2 up to 30 mM (Limami et al., 2008; Melo-Oliveira et al., 1996; Skopelitis et al., 2007; Tercé-Laforgue, Dubois, et al., 2004; Tercé-Laforgue, Mäck, et al., 2004), the concentration of 5 mM was chosen for our experimental setups. Cultures were obtained by seeding gemmae, or seeds, in the case of Arabidopsis, grown in the presence or absence of 5 mM NH_4^+ and maintained in the same conditions for 30 days, as well as cultures germinated and grown 14 days in absence of NH_4^+ then shifted on 5 mM NH_4^+ supplied medium, were analyzed. The NAD-dependent aminating activity of GDH was revealed by native-PAGE of protein extracts followed by in gel staining. Relative abundance and post-translational modification pattern of GDH protein were assayed in total protein extracts subjected to mono- and two-dimensional Western Blot analyses (Figure 7). The first visible effect of ammonium deprivation was witnessed on Arabidopsis electrophoretic patterns (Figure 7A): a decrease in the relative abundance of anodal GDH isoforms was detected, indicating that a selective decrease of α subunits occurred that affected the assembly of α homo- and heterohexamers. On the contrary, no modifications of the isoenzymatic GDH profile were observed for *L. cruciata*, *M. polymorpha*, and *C. fissa*, which showed a single-band pattern. As the plant material was collected in the natural environment, this seemed to exclude the presence of heteromeric isoforms differently expressed depending on the growth conditions applied here. According to the NAD-dependent in gel staining, the presence of ammonium excess led to a significant increase of the GDH aminating activity in all the species analyzed: GDH total activity in Arabidopsis plants grown for 30 days in the presence of 5 mM NH_4^+ was found to be 13.7-fold higher than the control. The same was

observed in ammonium-exposed *L. cruciata*, *M. polymorpha*, and *C. fissa* cultures, whose GDH activities were found to be 5.6-, 1.2-, and 3.2-fold higher, respectively.

A higher relative abundance of GDH protein was found in treated cultures when compared to controls in all the species considered (Figure 7B), albeit in Arabidopsis it apparently did not correspond to the difference recorded for the enzyme activity (1.9 vs. 13.7 folds, respectively). The analysis of 2D-WB patterns provided interesting outcomes: a general up-regulation of all the protein isoforms present in the NH_4^+ -depleted medium was obtained when plants are grown in a condition of continuous exposure to ammonium (Figure 7C), and the appearance of additional, more acidic signals in *C. fissa* was observed. Interestingly, in Arabidopsis, the increase of secondary spot intensities detected in 5 mM NH_4^+ cultures was accompanied by a decrease of the main GDH isoform, which suggested a compensatory mechanism.

Similar results were found when *M. polymorpha* and *C. fissa* cultures were transferred on 5 mM NH_4^+ after an initial growth phase of ammonium depletion: after the nutritional shift, an increase in GDH activity of 1.1 and 1.8 folds, respectively was observed, accompanied by an increase of the 1D-WB signal intensity (Figure S2). However, while in *C. fissa* the difference between the protein relative abundance in treated and untreated samples decreased from 7.8 to 2.9 folds, in 30-day exposed and 7-day exposed cultures, respectively, in *M. polymorpha* it surprisingly increased from 1.4 to 6.4 folds.

3.5 | Targeted metabolomics analysis in *M. polymorpha* and *C. fissa* exposed to ammonium showed different amino acid profiles

In order to unravel the effect of ammonium excess on the amino acid profile, water extracts from cultures of Arabidopsis, *M. polymorpha* and *C. fissa* cultivated in vitro and grown 30 days in absence or presence of 5 mM NH_4^+ were subjected to a targeted LC-MS analysis. All the protein amino acids were detected by the targeted metabolomics analysis, except for valine, cysteine, alanine, and glycine. The 2-oxoglutarate content was investigated as well (Figure 8). Amongst amino acids, histidine and arginine increased in all the three species, whereas a reduction in the content of 2-oxoglutarate was observed. The exposure to ammonium induced an augmentation in tryptophan and asparagine levels in Arabidopsis, whereas the content of the former was lower in *C. fissa*. Lysine and proline were most abundant in *M. polymorpha* and *C. fissa*, respectively. On the contrary, a decrease of the glutamate amount was detected in both *M. polymorpha* and Arabidopsis, but not in *C. fissa*.

Interestingly, the response to ammonium exposure in terms of glutamine content proved to be the most different within the three species, as the NH_4^+ excess determined a strong augmentation in Arabidopsis, a reduction in *C. fissa* and no significant differences in *M. polymorpha*.

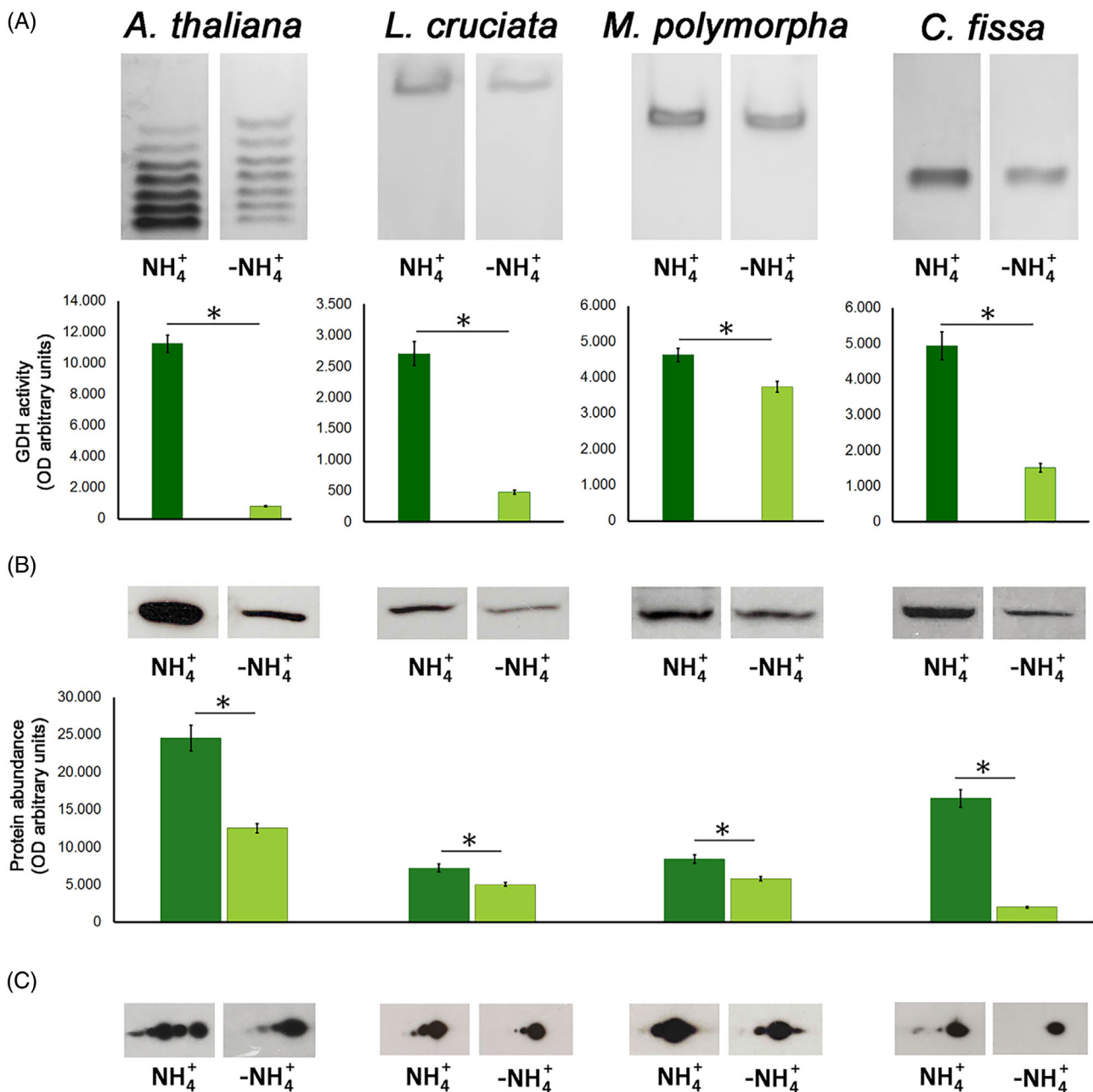


FIGURE 7 Effect of 5 mM NH₄⁺ on GDH activity and electrophoretic profile in *Arabidopsis*, *L. cruciata*, *M. polymorpha* and *C. fissa*. (A) GDH in gel activity, (B) protein abundance and (C) post-translational pattern were determined in axenic plant cultures grown and maintained for 30 days in NH₄NO₃-free MS medium either supplied with 5 mM ammonium (NH₄⁺) or not (-NH₄⁺). Equal quantity of total proteins was loaded for each sample (20 µg for native-PAGE, 15 µg for 1D-WB and 125 µg for 2D-WB). Data are the result of densitometric analyses conducted on acquired gel or autoradiographic film images and are reported as means of technical replicates ($n = 3$) ± SD. Significant differences between means were determined by Student's *t*-test (* $p < 0.05$). Experiments were conducted in three biological independent replicates.

3.6 | GDH activity was not found differentially distributed at a tissue level, while at subcellular level the protein proved to be strictly associated with the plastid endomembrane system

To approximately detect how GDH activity could be allocated in the liverworts body, and in turn to have a clue of a possible differential distribution of the enzyme within tissues independently of a variable

ammonia supplementation, an in vivo staining protocol was applied on *M. polymorpha* axenic fresh tissues sampled from 30 days-old cultures grown on complete, half-strength MS medium. The staining procedure, that successfully allowed to directly spot the GDH activity in *Arabidopsis* in planta (Marchi et al., 2021), was effective in detecting the GDH activity in liverwort species as well (Figure 9A). No color development was observed in tissues infiltrated with the reaction mixture deprived of glutamate while a strong and

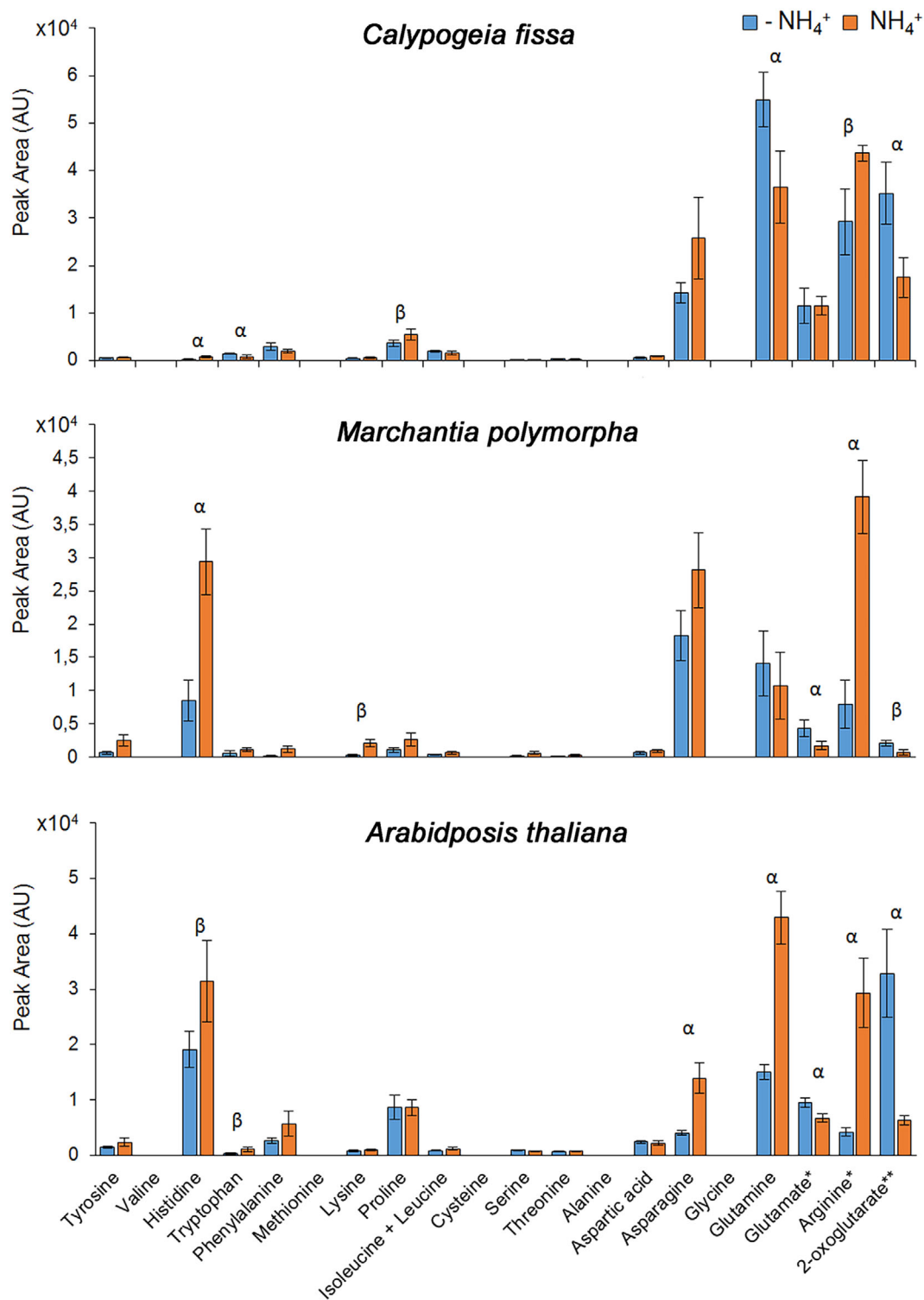


FIGURE 8 Amino acids profiles in *Arabidopsis*, *M. polymorpha* and *C. fissa* cultures in response to ammonium depletion or excess. Plant cultures were grown and maintained for 30 days in NH_4NO_3 -free MS medium either supplied with 5 mM ammonium (NH_4^+) or not ($-NH_4^+$). Values for glutamic acid and arginine were assessed in samples diluted 1:50, whereas all other amino acids are showed for samples diluted 1:10. Data are expressed as peak area in arbitrary units (AUs) and were obtained through LC-MS analysis performed in positive ionization, except for 2-oxoglutarate that was ionized in negative modality. Data are mean \pm SD ($n = 3$). A *t*-test was carried for each amino acid: α and β highlighted those amino acid with a $p < 0.01$ and $p < 0.05$, respectively.

homogenous staining of lobes and rhizoids was detected, suggesting that adult, fully differentiated individuals of *M. polymorpha* do not possess a peculiar organ/tissue-dependent pattern of GDH activity.

To determine the subcellular localization of the GDH protein, immunogold localization assays were conducted on lobe tissue of *M. polymorpha* grown 30 days onto complete, half-strength MS plates,

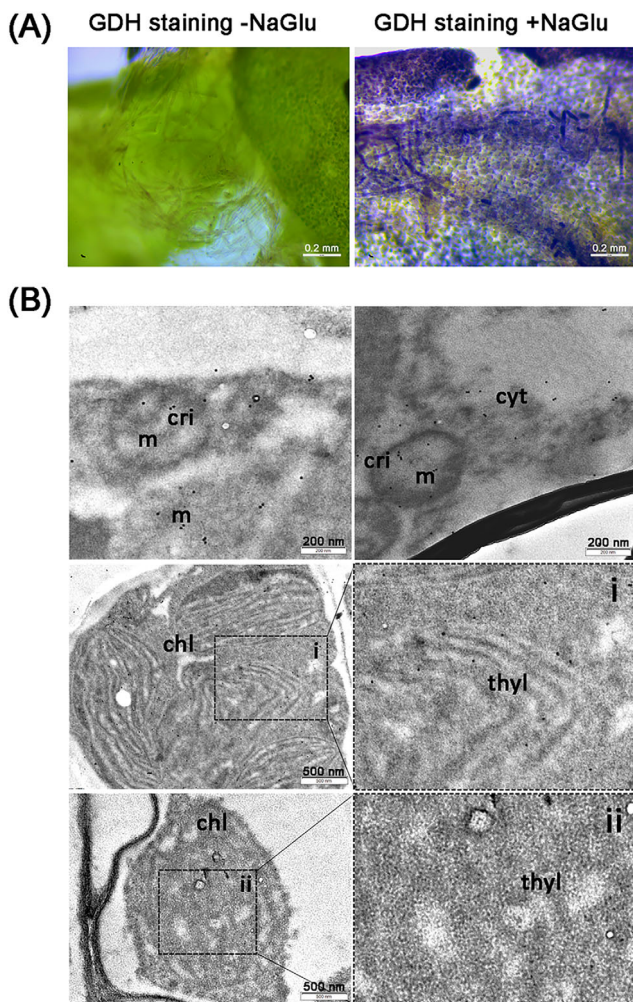


FIGURE 9 Distribution of GDH activity and enzyme in *M. polymorpha*. Fresh lobes from axenic cultures of *M. polymorpha* grown 30 days on complete, half-strength MS medium were subjected to an *in vivo* coloration for the detection of NAD-dependent GDH activity (A). Tissues treated at 70°C to inactivate enzymatic GDH-nondependent activities were vacuum-infiltrated with the staining mixture and incubated at 37°C (GDH staining +NaGlu). Staining with a reaction mixture deprived of Na-glutamate was used as GDH specificity control (GDH staining –NaGlu). Images were acquired with a stereo microscope (scale bar: 0.2 mm). Tissues from same cultures were subjected to immunogold electron microscopy to localize the enzyme at subcellular level (B). Gold particles (black dots) indicate the presence of GDH protein particularly associated to mitochondria (m) cristae (cri) and chloroplasts (chl) thylacoids (thyl).

using the same antibody exploited for Western Blot analyses. Specific reactive signals were detected in both mitochondria and chloroplasts (Figure 9B), as reported in previous studies conducted on Arabidopsis and other flowering plants (Fontaine et al., 2012). No labeling was observed in parenchyma cells when sections were incubated with pre-immune serum (Figure 9B, lower row). However, at more accurate examination, it has been revealed that the gold particles not simply localized in organelles whilst very rarely immunolocalization signals were detected in the vacuole or cytosol; instead, their presence was

strictly associated with the cristae and thylakoids of mitochondria and chloroplasts, respectively.

4 | DISCUSSION

4.1 | Liverworts GDH enzyme is consistent with a 6 α homohexamer encoded by a single gene whose ancestor diverged into GDH1 and GDH2 in vascular plants

In this study, different techniques have been chosen to complement each other in investigating some structural and biochemical properties of the GDH enzyme in selected liverwort species. Phenotypic analysis conducted on the native electrophoretic patterns, immunochemical assays performed on protein extracts and the examination of the amino acid sequence support the hypothesis of a unique GDH isoenzyme in liverworts, composed by the association of identical subunits encoded by a single gene. This observation suggests that the common ancestor shared between angiosperms and liverworts possessed a single GDH isoenzyme that diverged into GDH1 and GDH2 as a consequence of a whole genome duplication that occurred only in the vascular plants lineage (Linde et al., 2023). The analysis of amino acid sequences revealed a slightly higher similarity of the liverworts GDH protein to Arabidopsis GDH2 (corresponding to α subunit) rather than GDH1 (corresponding to β subunit). This is not in contrast with the detection of a single band in a more anodal position of the zymogram than the corresponding 6 α isoform of *A. thaliana*. Tercé-Laforgue and co-workers already reported that in *N. plumbaginifolia* the 6 α homohexamer localizes at level of the fifth band (from the cathode) of Arabidopsis electrophoretic pattern (Tercé-Laforgue et al., 2015).

Interestingly, the C-terminus of the protein was found to carry two residues that apparently draw a distinction within liverworts and between liverworts and vascular species: residue G391, shared by vascular species, *L. cruciata*, *M. polymorpha*, *C. conicum*, *Pellia* sp., and *C. fissa*, has been found as A391 in the two *Porellales*, while residue N398, that is conserved in Arabidopsis, *N. plumbaginifolia*, and other 15 higher plant species, was substituted by G398 in all the liverwort species analyzed. In their previous work, Marchi and colleagues already reported this substitution for the glutamate dehydrogenase B-like gene of the moss *Physcomitrium patens* (*Physcomitrium patens*, Sequence ID: XP_024382943.1; Marchi et al., 2014).

The presence of additional, organ-specific isoforms possibly deriving from the association of different gene products preferentially expressed in diverse tissues (Marchi et al., 2013; Qiu et al., 2009) has been excluded by dissecting *M. polymorpha*, *L. cruciata*, and *C. conicum* gametophytes and/or sporophytes, and analyzing their native electrophoretic profile. GDH-immunoreactive clusters clearly indicated that different post-translational modifications occurred to the basic isoform of the protein, as the separation by isoelectrofocusing prior to two-dimensional gel electrophoresis and Western blotting enables the individual detection of alternative protein species with the same specific antibody (Herzog et al., 2020).

4.2 | The GDH protein is characterized by a significant resistance to thermal inactivation that varies upon species

Evidence from thermal inactivation experiments was also consistent with the proposition of an α homohexameric form, as in *Arabidopsis* the 6α homohexamer was found more thermosensitive than the 6β counterpart, particularly in root extracts (Marchi et al., 2014). On the other hand, according to the theoretical model of the protein GDH3 structure, the substitution of Ala411 at the C-term with the more hydrophobic Ser411 was suggested to affect the protein thermal stability. Therefore, the presence of A411 in *Arabidopsis* GDH1 and GDH2, *N. plumbaginifolia* GDHA and GDHB, and in the GDH-putative sequences of *L. cruciata*, *M. polymorpha*, *C. conicum*, *C. fissa*, *R. lindenbergiana*, and *Frullania* sp. are consistent with a robust interaction with the C-term helix with the opposite β A- β B loop at the subunits interface (Marchi et al., 2014).

Conversely, the G398N substitution might partially explain the difference of enzyme thermosensitivity between vascular and bryophytes species, as our results showed that it has been predicted to decrease the protein stability under thermal denaturation.

The existence of GDH isoenzymes differently prone to thermal inactivation in different tissues was usually ascribed to heterohexameric isoforms, as the subunit arrangements vary depending on the differential expression of coding genes. A paradigmatic example is provided by the human GDH (Shashidharan et al., 1997; Shashidharan & Plaitakis, 2014). Coherently with the hypothesis of a unique homohexameric enzyme, when we assessed the thermostability of the GDH enzyme in different organs/tissues of *M. polymorpha*, our expectations have been confirmed by our results.

Besides the undoubtful relevance that the ability of a protein to maintain its structural stability under high temperature exposure should represent for thermotolerant organisms, the peculiar resistance that characterizes GDH isoenzymes in various mesophilous plant species such as *Arabidopsis*, is still fascinating, also due to scientific speculations about its evolutionary implications: as a protein's thermal stability relies on the kinetics and energetics of changes in its three-dimensional conformation, it is not so bizarre to assume that during the organisms evolution their proteome should have proceeded to warrant protein functions at their physiological temperature along with its mechanisms of regulation. On the other hand, even considering that plants are exposed to wide temperature fluctuations and it is thus rational to expect that they have developed an adequate thermal stability to maintain the protein functions under variable environmental conditions, the comprehension of how key enzymes have been evolved during and after terrestrialization to operate in the most energetically efficient way is not trivial (Guihur et al., 2020). The incredible thermostability found in *Arabidopsis* did not characterize the GDH of liverwort species analyzed here, in which the enzyme activity seemed to be more affected by temperature even if lesser than in other plant species (Ehmke et al., 1984; Magalhaes et al., 1976). However, differences showed to be more likely species-specific than order-specific, supporting the hypothesis that GDH thermotolerance could have

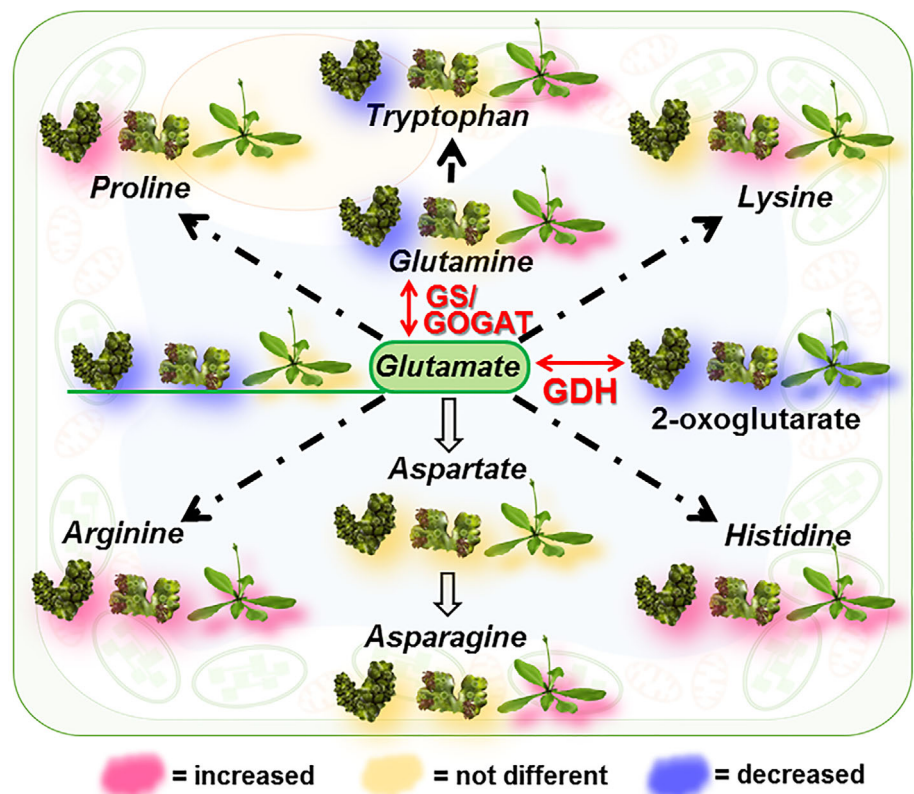
acted, and still acts, at different levels during the evolution of this vascular plant's sister group.

What has been observed for *C. fissa*, whose GDH thermosensitivity changed when assayed in extracts from wild or in vitro cultured plants, was not completely unexplained, as the developmental stage, as well as seasonal conditions, might act on the post-translational pattern of modifications, affecting the stability of the protein scaffold (Friso & van Wijk, 2015). The alteration of the electrophoretic positioning of GDH signals observed after thermal treatment of native extracts from individuals grown both in the natural environment and in vitro, might depend on the molecular interaction between subunits and mainly on their post-translational modification patterns. Functionally-relevant phosphorylation sites in particular are recognized to trigger conformational changes to proteins, regulating their molecular interactions and therefore modulating the peptide thermal stability. It should also be considered that in a native PAGE proteins are separated according to their charge, mass, and three-dimensional structure, and electrophoretic migration occurs because of the net negative charge retained by proteins in alkaline running buffers: at the same molecular weight, the higher the negative charge density the faster a protein will migrate. Additionally, the thermal treatment applied to plant extracts could have led to the degradation, detachment or re-arrangement of functional groups, with a consequent alteration of the protein surface charge. Hence, differences observed in the positioning of GDH signals might rely on different post-translational modification patterns, resulting in both different electrophoretic migration rate and enzyme thermosensitivity (Potel et al., 2021). In addition, the variability in the 2D-WB pattern could be perceived as species-dependent to some extent: for example, the single-spot pattern found in *P. epiphylla* seems to suggest that the regulation of GDH in this species could be untied from the protein post-translational modifications observed in other liverworts analyzed.

4.3 | Enzyme activity in liverworts is modulated by ammonium excess as in vascular plants

According to the existent literature the type of nitrogen source is one of the crucial exogenous factors involved in the modulation of GDH activity in plants, even if sometimes contrasting results concerning the possible catabolic versus anabolic role of GDH have been provided (Miyashita & Good, 2008). Despite that it has been well established that the enzyme should play a negligible role in the assimilation of ammonium, there is mounting evidence that its synthesis is enhanced by NH_4^+ concentration exceeding a certain threshold to provide 2-oxoglutarate in conditions of limiting carbon, and that the enzyme might act as a sensor to evaluate the metabolic status of the plant with respect to ammonium and sugar concentrations (Fontaine et al., 2012). This sensing has been proposed to specifically occur at the phloem level in vascular plants, as the GDH protein demonstrated to be mainly localized in the phloem companion cells (Dubois et al., 2003; Fontaine et al., 2006; Fontaine et al., 2012) in whose mitochondria and cytosol its amount increases in response to NH_4^+ excess (Tercé-Laforgue, Dubois,

FIGURE 10 Simplified depiction of amino acid biosynthetic pathways involving Glutamate and referring to *C. fissa*, *M. polymorpha* and *Arabidopsis* (from the left) exposed to ammonium. GS/GOGAT- and GDH-dependent reactions are bolded in red. Dashed arrows: multiple step reactions. Full arrows: single step reactions. According to amino acid profiling, the colors indicate the level of the specific amino acids in cultures grown for 30 days in 5 mM NH_4^+ , with respect to not-treated cultures (blue: increased level; red: decreased level; yellow: no differences).



et al., 2004; Tercé-Laforgue, Mäck, et al., 2004). Our study highlighted how the ammonium-dependent up-regulation of the enzyme activity, that correlate with an increase of protein abundance, is admittedly disengaged from the presence of a phloem stream, as liverworts lack a proper vascular system. As metabolites might be transported within gametophytes through a translocation process based on plasmodesmata, this cell-to-cell transfer could explain the lack of a tissue-dependent activity in bryophytes. Consistently, the “sensor hypothesis” provided for vascular plants might be extended to this sister group, where, even if in absence of specialized conducting tissue, GDH could still act as a sensor of the metabolic status of the plant.

The response of *L. cruciata*, *M. polymorpha*, and *C. fissa* under ammonium excess and sucrose reduction showed to confirm what is observed in vascular plants, in which NH_4^+ accumulation in aging leaves is associated with a carbohydrate/energy depletion during senescence and was reported to stimulate GDH activity (Restivo, 2004; Suarez et al., 2002; Titus & Kang, 1982). This finding suggests that in both vascular species and liverworts a carbon/nitrogen stress condition possibly inactivates the prominent NH_4^+ assimilatory/detoxifying pathway represented by GS/GOGAT, a situation that imposes the necessity for a complementary pathway for the organism to survive and results in a GDH activity stimulation. More notably, the augmentative effect that NH_4^+ exerts on GDH activity in *L. cruciata*, *M. polymorpha* and *C. fissa* is in accordance with the increase of α -predominant heterohexamers observed in the zymogram profile of *Arabidopsis* (Figure 7A), and it is also consistent with the up-regulation of *GDHA* gene expression

recorded in *N. plumbaginifolia* calli exposed to an ammonium enriched medium (Restivo, 2004). With regard to the difference in terms of GDH activity magnitude and relative protein abundance in NH_4^+ treated liverworts and *Arabidopsis*, it should be however considered that while some enzyme isoforms can be easily observed separately in zymograms, single subunits are forced to co-migrate in 1D-WB, due to the limitations of mono-dimensional SDS-PAGE resolving properties, and their contribution to the signal's extent during immunodetection can be affected by a sort of “shielding effect.”

When studies about the overexpression of *N. plumbaginifolia* *GDHA* and *GDHB* genes in *N. tabacum* demonstrated an up-regulation of GDH activity and an accumulation of asparagine accompanied by a decrease in glutamate, glutamine, and proline content (Tercé-Laforgue et al., 2013), it was speculated that metabolic perturbation induced by GDH overexpression could preferentially redirect glutamine toward asparagine biosynthesis, determining in turn a reduction in proline of which glutamate and glutamine are substrates (Brugière et al., 1999; Forde & Lea, 2007). However, despite that it would represent an attractive hypothesis to find correspondence within liverworts as well, our results showed that for a number of amino acids the accumulation pattern was different according either to species examined, or ammonia exposure. The most interesting outcome regarded the different perturbation extent of glutamate, glutamine, arginine and asparagine in *Arabidopsis*, *M. polymorpha*, and *C. fissa*, while the significant decrease observed for 2-oxoglutarate in all the three species has been ascribed to the increase of the GDH aminating activity.

By considering the amino acid biosynthetic pathways and the amino acid trends, our observations suggest that *C. fissa*, *M. polymorpha* and *Arabidopsis* could respond to the excess of ammonium by following different strategies (Figure 10). Arginine and histidine in particular increased in all the three species, suggesting that the excess of NH_4^+ might be stored in these final reaction products as well. On the contrary, the values of 2-oxoglutarate decreased in all species consistently with its role as precursor of glutamate for both GOGAT and GDH pathways (Liu et al., 2022).

4.4 | In *M. polymorpha*, the GDH-dependent activity is uniformly dispersed in the parenchyma, but the enzyme is preferentially associated with the mitochondria and plastids endomembrane system

Our investigations showed that *M. polymorpha* did not exhibit GDH activity in specific regions of the thallus, being in contrast with vascular species in which the enzyme was preferentially reported in the neighborhood of the phloem. With this regard, we found particularly interesting the detection of a significant GDH activity in rhizoids that was not different from what obtained in other tissues, an observation that raised stimulating evolutionary speculations about the relationship between these primitive structures and the root apparatus of higher plants. Regarding the subcellular localization of GDH and its isoforms, only a few direct outcomes by immunogold transmission electron microscopy were available, and were only referred to *Arabidopsis* (Fontaine et al., 2012) and crops such as maize (Dubois et al., 2003), wheat (Kichey et al., 2005), grapes (Paczek et al., 2002), and *Nicotiana* (Dubois et al., 2003; Fontaine et al., 2006; Tercé-Laforgue et al., 2013; Tercé-Laforgue, Dubois, et al., 2004; Tercé-Laforgue, Mäck, et al., 2004). Nevertheless, to uncover the actual site of action of a specific enzyme it is as essential to understand its physiological role in the organism's economy as the definition of its genetic and biochemical features. Having found GDH particles associated to chloroplasts and mitochondria inner membranes in *M. polymorpha* led to assume that key enzymes for amino acids metabolism and critical steps for nitrogen assimilation occur in plastids of Marchantiophyta as already demonstrated for angiosperms and algae (Masclaux-Daubresse et al., 2010; Sanz-Luque et al., 2015). This could be speculatively ascribed more to the single origin through primary endosymbiosis of plantae plastids rather than the recruitment of non-cyanobacterial enzymes during the early evolution of the plastid proteome.

5 | CONCLUSIONS

In 2003 Dubois and co-workers titled their review “Glutamate dehydrogenase in plants: is there a new story for an old enzyme?,” making a considerable effort to take stock of the situation about the involvement of this ancient enzyme in governing inorganic nitrogen assimilation in higher plants. Despite the solid outcomes they provided about

GDH localization at both tissue and cell level, physiological and developmental processes in which the enzyme occupy a leading role, and major drawbacks affecting the predictability of experimental results (Dubois et al., 2003), they left us with the consciousness of how many question marks are to be solved yet. One above all is why the cell relies on GDH to deaminate glutamate when it has been repeatedly observed that where an ammonium increase occurs, an increase of isocitrate dehydrogenases is also induced, which replenishes the carbohydrate shortage by releasing α -ketoglutarate (Ferrario-Mery et al., 2002; Lancien et al., 1999). The metabolic role of GDH isoenzymes should not be assumed as simply correlated with the ammonium assimilation or the carbon skeleton generation, but rather perceived as the cells multileveled purpose to reach the most efficient balance between C and N status. Hence, answers about its great and so widely conserved thermostability, as well as how do its structure and biochemical features cope with the environmental constraints characterizing the most different plant habitats and the role that it possibly played during the successful terrestrialization must be achieved.

Although many aspects of the significance that GDH plays in vascular plants have been clarified, others could still emerge from comparative biology studies: for example, cross-lineage approaches might provide, if applied to bryophytes, decisive insights to unravel the phylogenetic history of this enzyme within green plants taxa. According to our results, it can be reasonably suggested that the GDH isoenzyme in modern liverworts shares the same ancestor with a single GDH protein of vascular plants that has diverged into GDH1 and GDH2 following a whole genome duplication in the vascular plant lineage occurred after the evolutionary bifurcation that separated bryophytes and tracheophytes (Puttick et al., 2018). However, despite the speculation that the ancestral protein could share more biochemical properties with the modern GDH α isoenzyme, the patterns that drove its evolutionary trajectory from terrestrialization are far from being revealed.

The possibility to overexpress heterologous GDH genes from angiosperms in liverwort species and examine the GDH isoenzyme composition in transgenic plants should be pursued. This would provide highly fascinating cues about the function and interaction of GDH subunits, and possibly about structural features that confer its peculiar thermal stability to the GDH enzyme in plants. In this regard, further investigations should take in account that the results of studies carried on extracts from plants grown in vitro or in defined media can only be interpreted with care in the context of real-world environmental conditions. Factors such as cytoplasmic protein concentration, small molecule interactions and cellular localization can be expected to have significant effects on thermal stability and molecular interactions under different experimental conditions. Additional immunohistochemical analyses are also desirable, aimed at investigating if a tissue- or developmental stage-specific localization of the enzyme could be recognized in liverworts as well as other non-flowering species, and eventually leading to reconsider the vascular tissue as a key location for the GDH as a “metabolic sensor” role.

By shedding light on some structural and functional features of the glutamate dehydrogenase enzyme in liverworts, we believe this

research could significantly contribute to our understanding of how inorganic N is assimilated and managed in bryophytes and the possible declinations of N metabolism during plant terrestrialization.

AUTHOR CONTRIBUTIONS

Francesca Degola and Alessandro Petraglia conceptualized the study. Giorgio Chiari and Alessandro Petraglia retrieved the plant material and identified the species. Martina Brambilla and Francesca Degola managed and propagated the plant material, and performed the biochemical and functional analyses. Luca Nerva performed bioinformatics and data analyses. Mauro Commisso performed metabolome analyses. Rita Musetti conducted electron microscopy. Francesca Degola, Mauro Commisso, and Rita Musetti provided resources. Francesca Degola supervised the project development and wrote the original draft. Alessandro Petraglia edited the manuscript. All authors reviewed the article.

ACKNOWLEDGMENTS

Authors are indebted to Antonietta Cirasolo for her technical help in preparing culture media. Francesca Degola in particular is deeply grateful to Dr. Mauro Degola, for his loving support during the collection of liverworts wild material, and to Prof. Francesco M. Restivo, for everything he taught, he gave, he grew.

DATA AVAILABILITY STATEMENT

The data that support the findings of this study are available from the corresponding author upon reasonable request.

ORCID

Francesca Degola  <https://orcid.org/0000-0002-3937-251X>

REFERENCES

- Aubert, S.R., Bligny, R., Douce, R., Gout, E., Ratcliffe, R.G. & Roberts, J.K.M. (2001) Contribution of glutamate dehydrogenase to mitochondrial glutamate metabolism studied by C-13 and P-31 nuclear magnetic resonance. *Journal of Experimental Botany*, 52(354), 37–45.
- Barger, N.N., Weber, B., Garcia-Pichel, F., Zaady, E. & Benalp, J. (2016) Patterns and controls on nitrogen cycling of biological soil crusts. In: Weber, B., Büdel, B. & Benalp, J. (Eds.) *Biological soil crusts as an organizing principle in drylands*. Cham: Springer International Publishing, pp. 257–285.
- Baslerova, M. & Dvorakova, J. (1962) *Algarum, hepaticarum, Muscurumque in cultris collection*. NCSAV, Praha, p. 59.
- Benalp, J. (2001) Factors influencing nitrogen fixation and nitrogen release in biological soil crusts. In: Benalp, J. & Lange, O.L. (Eds.) *Biological soil crusts: structure, function, and management*. Berlin: Springer-Verlag Berlin Heidelberg, pp. 241–261.
- Bhadula, S.K. & Shargool, P.D. (1991) A plastidial localization and origin of L-glutamate dehydrogenase in a soybean cell culture. *Plant Physiology*, 95(1), 258–263.
- Bradford, M.M. (1976) A rapid and sensitive method for the quantitation of microgram quantities of proteins utilizing the principle of protein dye binding. *Analytical Biochemistry*, 72, 248–254.
- Britton, K.L., Baker, P.J., Rice, D.W. & Stillman, T.J. (1992) Structural relationship between the hexameric and tetrameric family of glutamate dehydrogenases. *European Journal of Biochemistry*, 209, 851–859.
- Brugère, N., Dubois, F., Limami, A., Lelandais, M., Roux, Y., Sangwan, R. et al. (1999) Glutamine synthetase in the phloem plays a major role in controlling proline production. *Plant Cell*, 11, 1995–2011.
- Degola, F., Sanità di Toppi, L. & Petraglia, A. (2022) Bryophytes: how to conquer an alien planet and live happily (ever after). *Journal of Experimental Botany*, 73, 4267–4272.
- Dubois, F., Tercé-Laforgue, T., Gonzalez-Moro, M.-B., Estavillo, J.-M., Sangwan, R., Gallais, A. et al. (2003) Glutamate dehydrogenase in plants: is there a new story for an old enzyme? *Plant Physiology and Biochemistry*, 41, 565–576.
- Ehmke, A., Scheid, H.W. & Hartmann, T. (1984) Glutamate dehydrogenase of *Pisum sativum*: heat-dependent interconversion of the multiple forms. *Zeitschrift für Naturforschung*, 39, 257–260.
- Ferrario-Mery, S., Hodges, M., Hirel, B. & Foyer, C.H. (2002) Photorespiration dependent increases in phosphoenolpyruvate carboxylase, isocitrate dehydrogenase and glutamate dehydrogenase in transformed tobacco plants deficient in ferredoxin-dependent glutamine-a-ketoglutarate amino transferase. *Planta*, 214, 877–886.
- Fischer, P. & Klein, U. (1988) Localization of nitrogen-assimilating enzymes in the chloroplast of *Chlamydomonas reinhardtii*. *Plant Physiology*, 88(3), 947–952.
- Fontaine, J.X., Saladino, F., Agrimonti, C. et al. (2006) Control of the synthesis and subcellular targeting of the two GDH genes products in leaves and stems of *Nicotiana glauca* and *Arabidopsis thaliana*. *Plant and Cell Physiology*, 47(3), 410–418. <https://doi.org/10.1093/pcp/pcj008>
- Fontaine, J.X., Terce-Laforgue, T., Armengaud, P., Clement, G., Renou, J.P., Pelletier, S. et al. (2012) Characterization of a NADH-dependent glutamate dehydrogenase mutant of *Arabidopsis* demonstrates the key role of this enzyme in root carbon and nitrogen metabolism. *Plant Cell*, 24(10), 4044–4065.
- Forde, B.G. & Lea, P.J. (2007) Glutamate in plants: metabolism, regulation, and signaling. *Journal of Experimental Botany*, 58(9), 2339–2358.
- Friso, G. & van Wijk, K.J. (2015) Posttranslational protein modifications in plant metabolism. *Plant Physiology*, 169(3), 1469–1487.
- Galvez, S., Lancien, M. & Hodges, M. (1999) Are isocitrate dehydrogenases and 2-oxoglutarate involved in the regulation of glutamate biosynthesis? *Trends in Plant Science*, 4(12), 484–490.
- Grzechowiak, M., Sliwiak, J., Jaskolski, M. & Ruskowski, M. (2020) Structural studies of Glutamate Dehydrogenase (Isoform 1) from *Arabidopsis thaliana*, an important enzyme at the branch-point between carbon and nitrogen metabolism. *Frontiers in Plant Science*, 11, 754–771.
- Guihur, A., Fauvet, B., Finka, A., Quadroni, M. & Goloubinoff, P. (2020) Quantitative proteomic analysis to capture the role of heat-accumulated proteins in moss plant acquired thermotolerance. *Plant, Cell and Environment*, 44(7), 2117–2133.
- Guo, S., Duan, J.A., Qian, D., Tang, Y., Qian, Y., Wu, D. et al. (2013) Rapid determination of amino acids in fruits of *Ziziphus jujuba* by hydrophilic interaction ultra-high-performance liquid chromatography coupled with triple-quadrupole mass spectrometry. *Journal of Agricultural and Food Chemistry*, 61(11), 2709–2719.
- Hall, T.A. (1999) BIOEDIT: a user-friendly biological sequence alignment editor and analysis program for windows 95/98/NT. *Nucleic Acids Symposium Series*, vol. 41, pp. 95–98.
- Heeschen, V., Gerendas, J., Richter, C.P. & Rudolph, H. (1997) Glutamate dehydrogenase of *Sphagnum*. *Phytochemistry*, 45, 881–887.
- Herzog, R., Wagner, A., Wrettos, G., Stampf, K., Bromberger, S., Sperl, E. et al. (2020) Improved alignment and quantification of protein signals in two-dimensional Western Blotting. *Journal of Proteome Research*, 9(6), 2379–2390.
- Igarashi, D., Izumi, Y., Dokiya, Y., Totsuka, K., Fukusaki, E. & Ohsumi, C. (2009) Reproductive organs regulate leaf nitrogen metabolism mediated by cytokinin signal. *Planta*, 229, 633–644.
- Ireland, R.J. & Lea, P.J. (1999) The enzymes of glutamine, glutamate, asparagine, and aspartate metabolism. In: Singh, B.K. (Ed.) *Plant amino acids*.

- Biochemistry and biotechnology*. New York: Marcel Dekker Inc, pp. 49–109.
- Kichey, T., Le Gouis, J., Sangwan, B., Hirel, B. & Dubois, F. (2005) Changes in the cellular and subcellular localization of glutamine synthetase and glutamate dehydrogenase during flag leaf senescence in wheat (*Triticum aestivum* L.). *Plant and Cell Physiology*, 46(6), 964–974.
- Kumar, S., Stecher, G., Li, M., Knyaz, C. & Tamura, K. (2018) MEGA X: molecular evolutionary genetics analysis across computing platforms. *Molecular Biology and Evolution*, 35(6), 1547–1549.
- Kwinta, J. & Bielawski, W. (1998) Glutamate dehydrogenase in higher plants. *Acta Physiologia Plantarum*, 20, 453–463.
- Lam, H.-M., Koschigano, K.T., Oliveira, I.C., Melo-Oliveira, R. & Coruzzi, G.M. (1996) The molecular-genetics of nitrogen assimilation into amino acids in higher plants. *Annual Review of Plant Physiology and Plant Molecular Biology*, 47, 569–593.
- Lancien, M., Ferrario-Méry, S., Roux, Y., Bismuth, E., Masclaux, C., Hirel, B. et al. (1999) Simultaneous expression of NAD-dependent isocitrate dehydrogenase and other Krebs cycle genes after nitrate resupply to short-term nitrogen starved *Nicotiana tabacum*. *Plant Physiology*, 120(3), 717–726.
- Lee, J.A. & Stewart, G.R. (1979) Ecological aspects of nitrogen assimilation. *Advances in Botanical Research*, 6, 1–43.
- Lehmann, T., Dabert, M. & Nowak, W. (2011) Organ-specific expression of glutamate dehydrogenase (GDH) subunits in yellow lupine. *Journal of Plant Physiology*, 168(10), 1060–1066.
- Lesk, A.M. (1995) NAD-binding domains of dehydrogenases. *Current Opinions in Structural Biology*, 5(6), 775–783.
- Limami, A.M., Glevarec, G., Ricoult, C., Cliquet, J.-B. & Planchet, E. (2008) Concerted modulation of alanine and glutamate metabolism in young *Medicago truncatula* seedlings under hypoxic stress. *Journal of Experimental Botany*, 59(9), 2325–2335.
- Linde, A.M., Singh, S., Bowman, J.L., Eklund, M., Cronberg, N. & Lagercrantz, U. (2023) Genome evolution in plants: complex thalloid liverworts (Marchantiopsida). *Genome Biology and Evolution*, 15(3), evad014.
- Liu, X., Hu, B. & Chu, C. (2022) Nitrogen assimilation in plants: current status and future prospects. *Journal of Genetics and Genomics*, 49(5), 394–404.
- Loulakakis, K.A. & Roubelakis-Angelakis, K.A. (1990) Immunocharacterization of NADH-glutamate dehydrogenase from *Vitis vinifera* L. *Plant Physiology*, 94(1), 109–113.
- Loulakakis, K.A. & Roubelakis-Angelakis, K.A. (1991) Plant NAD(H)-glutamate dehydrogenase consists of two subunit polypeptides and their participation in the seven isozymes occurs in an ordered ratio. *Plant Physiology*, 97(1), 104–111.
- Magalhaes, A.C., Peters, D.B. & Hageman, R.H. (1976) Influence of temperature on nitrate metabolism and leaf expansion in soybean (*Glycine max* L. Merr.) seedlings. *Plant Physiology*, 58, 12–16.
- Marchi, L., Degola, F., Baruffini, E. & Restivo, F.M. (2021) How to easily detect plant NADH-glutamate dehydrogenase (GDH) activity? A simple and reliable in planta procedure suitable for tissues, extracts and heterologous microbial systems. *Plant Science*, 304, 110714.
- Marchi, L., Degola, F., Polverini, E., Tercé-Laforgue, T., Dubois, F. & Hirel, B. (2013) Glutamate dehydrogenase isoenzyme 3 (GDH3) of *Arabidopsis thaliana* is regulated by a combined effect of nitrogen and cytokinin. *Plant Physiology and Biochemistry*, 73, 368–374.
- Marchi, L., Polverini, E., Degola, F., Baruffini, E. & Restivo, F.M. (2014) Glutamate dehydrogenase isoenzyme 3 (GDH3) of *Arabidopsis thaliana* is less thermostable than GDH1 and GDH2 isoenzymes. *Plant Physiology and Biochemistry*, 83, 225–231.
- Masclaux-Daubresse, C., Daniel-Vedele, F., Dechorgnat, J., Chardon, F., Gaufichon, L. & Suzuki, A. (2010) Nitrogen uptake, assimilation and remobilization in plants: challenges for sustainable and productive agriculture. *Annals of Botany*, 105(7), 1141–1157.
- Meade, R. (1984) Ammonia-assimilating enzymes in bryophytes. *Physiologia Plantarum*. 60(3), 305–308. <https://doi.org/10.1111/j.1399-3054.1984.tb06067.x>
- Melo-Oliveira, R., Oliveira, I.C. & Coruzzi, M.-G. (1996) *Arabidopsis thaliana* mutant analysis and gene regulation defines a nonredundant role for glutamate dehydrogenase in nitrogen assimilation. *Proceedings of the National Academy of Sciences of the United States of America*, 93(10), 4718–4723.
- Mifflin, B.J. & Habash, D.Z. (2002) The role of glutamine synthetase and glutamate dehydrogenase in nitrogen assimilation and possibilities for improvement in the nitrogen utilization of crops. *Journal of Experimental Botany*, 53, 979–987.
- Mifflin, B.J. & Lea, P.J. (1980) Ammonia assimilation. In: Mifflin, B.J. (Ed.) *The biochemistry of plants*, Vol. 5. New York: Academic Press, pp. 169–202.
- Miyashita, Y. & Good, A.G. (2008) NAD(H)-dependent glutamate dehydrogenase is essential for the survival of *Arabidopsis thaliana* during dark-induced carbon starvation. *Journal of Experimental Botany*, 59(3), 667–680.
- Musetti, R., Carraro, L., Loi, N. & Ermacora, P. (2002) Application of immunoelectron microscopy techniques in the diagnosis of phytoplasma diseases. *Microscopy Research and Techniques*, 56(6), 462–464.
- Oaks, A. & Hirel, B. (1985) Nitrogen metabolism in roots. *Annual Review of Plant Physiology*, 36, 345–365.
- Ohshima, T. & Nishida, N. (1993) Purification and properties of extremely thermostable glutamate dehydrogenase from two hyperthermophilic Archeobacteria, *Pyrococcus woesei* and *Pyrococcus furiosus*. *Bioscience Biotechnology Biochemistry*, 57(6), 945–951.
- Oliveira, M.F. & Maciel-Silva, A.S. (2022) Biological soil crusts and how they might colonize other worlds: insights from these Brazilian ecosystem engineers. *Journal of Experimental Botany*, 73(13), 4362–4379.
- Paczek, V., Dubois, F., Sangwan, R., Morot-Gaudry, J.-F., Roubelakis-Angelakis, K.A. & Hirel, B. (2002) Cellular and subcellular localisation of glutamine synthetase and glutamate dehydrogenase in grapes gives new insights on the regulation of carbon and nitrogen metabolism. *Planta*, 216, 245–254.
- Pan, Y., Li, J., Li, X., Chen, J. & Bai, G. (2014) Determination of free amino acids in isatidis radix by HILIC-UPLC-MS/MS. *Bulletin of the Korean Chemical Society*, 35(1), 197–203.
- Parthiban, V., Gromiha, M.M., Abhinandan, M. & Schomburg, D. (2007) Computational modeling of protein mutant stability: analysis and optimization of statistical potentials and structural features reveal insights into prediction model development. *BMC Structural Biology*, 7, 54.
- Parthiban, V., Gromiha, M.M., Hoppe, C. & Schomburg, D. (2007) Structural analysis and prediction of protein mutant stability using distance and torsion potentials: role of secondary structure and solvent accessibility. *Proteins*, 17(4), 355–362.
- Parthiban, V., Gromiha, M.M. & Schomburg, D. (2006) CUPSAT: prediction of protein stability upon point mutations. *Nucleic Acids Research*, 34 (Web Server issue), W239–W242.
- Pavesi, A. (2014) Prediction of the determinants of thermal stability by linear discriminant analysis: the case of the glutamate dehydrogenase protein family. *J Theor Biol*, 357, 160–168. <https://doi.org/10.1016/j.jtbi.2014.05.013>
- Pavesi, A., Ficarelli, A., Tassi, F. & Restivo, F.M. (2000) Cloning of two glutamate dehydrogenase cDNAs from *Asparagus officinalis*: sequence analysis and evolutionary implications. *Genome*, 43(2), 306–316.
- Potel, C.M., Kurzawa, N., Becher, I., Typas, A., Mateus, A. & Savitski, M.M. (2021) Impact of phosphorylation on thermal stability of proteins. *Nature Methods*, 18(7), 757–759.
- Puttick, M.N., Morris, J.L., Williams, T.A., Cox, C.J., Edwards, D., Kenrick, P. et al. (2018) The interrelationships of land plants and the nature of the ancestral embryophyte. *Current Biology*, 28(5), 733–745.
- Qiu, X., Xie, W., Lian, X. & Zhang, Q. (2009) Molecular analyses of the rice glutamate dehydrogenase gene family and their response to nitrogen and phosphorous deprivation. *Plant Cell Reports*, 28, 1115–1126.

- Restivo, F.M. (2004) Molecular cloning of glutamate dehydrogenase genes of *Nicotiana plumbaginifolia*: structure analysis and regulation of their expression by physiological and stress conditions. *Plant Science*, 166, 971–982.
- Sanz-Luque, E., Chamizo-Ampudia, A., Llamas, A., Galvan, A. & Fernandez, E. (2015) Understanding nitrate assimilation and its regulation in microalgae. *Frontiers in Plant Science*, 6, 899.
- Shashidharan, P., Clarke, D.D., Ahmed, N., Moschonas, N. & Plaitakis, A. (1997) Nerve tissue-specific human glutamate dehydrogenase that is thermolabile and highly regulated by ADP. *Journal of Neurochemistry*, 68(5), 1804–1811.
- Shashidharan, P. & Plaitakis, A. (2014) The discovery of human of GLUD2 glutamate dehydrogenase and its implications for cell function in health and disease. *Neurochemical Research*, 39(3), 460–470.
- Skopelitis, D.S., Paranychianakis, N.V., Kouvarakis, A., Spyros, A., Stephanou, E.G. & Roubelakis-Angelakis, K.A. (2007) The isoenzyme 7 of tobacco NAD(H)-dependent glutamate dehydrogenase exhibits high deaminating and low aminating activities in vivo. *Plant Physiology*, 145(4), 1726–1734.
- Song, L., Lu, H.Z., Xu, X.L., Su, L., Shi, X.M., Chen, X. et al. (2016) Organic nitrogen uptake is a significant contributor to nitrogen economy of subtropical epiphytic bryophytes. *Scientific Reports*, 6, 30408.
- Srivastava, H.S. & Singh, R.P. (1987) Role and regulation of L-glutamate dehydrogenase activity in higher plants. *Phytochemistry*, 26(3), 597–610.
- Stewart, G.R., Mann, A.F. & Fentem, P.A. (1980) Enzymes of glutamate formation: glutamate dehydrogenase, glutamine synthetase and glutamate synthase. In: Mifflin, B.J. (Ed.) *The biochemistry of plants*, Vol. 5. New York: Academic Press, pp. 271–327.
- Stewart, G.R., Shatilov, V.R., Turnbull, M.H., Robinson, S.A. & Goodall, R. (1995) Evidence that glutamate dehydrogenase plays a role in the oxidative deamination of glutamate in seedlings of *Zea mays*. *Australian Journal of Plant Physiology*, 22(5), 805–809.
- Suarez, M.F., Avila, C., Gallardo, F., Canton, F.R., Garcia-Gutierrez, A., Claros, M.G. et al. (2002) Molecular and enzymatic analysis of ammonium assimilation in woody plants. *Journal of Experimental Botany*, 53(370), 891–904.
- Syntichaki, K.M., Loulakakis, K.A. & Roubelakis-Angelakis, K.A. (1996) The amino-acid sequence similarity of plant glutamate dehydrogenase to the extremophilic archaeal enzyme conforms to its stress-related function. *Gene*, 168(1), 87–92.
- Temple, S.J., Vance, C.P. & Gantt, J.S. (1998) Glutamate synthase and nitrogen assimilation. *Trends in Plant Science*, 3(2), 51–56.
- Tercé-Laforgue, T., Bedu, M., Dargel-Grafin, C., Dubois, F., Gibon, Y., Restivo, F.M. et al. (2013) Resolving the role of plant glutamate dehydrogenase: II. Physiological characterization of plants overexpressing the two enzyme subunits individually or simultaneously. *Plant and Cell Physiology*, 54(10), 1635–1647.
- Tercé-Laforgue, T., Clément, G., Marchi, L., Restivo, F.M., Lea, P.J. & Hirel, B. (2015) Resolving the role of plant NAD-glutamate dehydrogenase: III. Overexpressing individually or simultaneously the two enzyme subunits under salt stress induces changes in the leaf metabolic profile and increases plant biomass production. *Plant and Cell Physiology*, 56(10), 1918–1929.
- Tercé-Laforgue, T., Dubois, F., Ferrario-Méry, S., Pou de Crezenzo, M.A., Sangwan, R. & Hirel, B. (2004) Glutamate dehydrogenase of tobacco (*Nicotiana tabacum* L.) is mainly induced in the cytosol of phloem companion cells when ammonia is provided either externally or released during photorespiration. *Plant Physiology*, 136(4), 4308–4317.
- Tercé-Laforgue, T., Mäck, G. & Hirel, B. (2004) New insights towards the function of glutamate dehydrogenase revealed during source-sink transition of tobacco (*Nicotiana tabacum*) plants grown under different nitrogen regimes. *Physiologia Plantarum*, 120(2), 220–228.
- Thurman, D.A., Palin, C. & Laycock, M.V. (1965) Isoenzymatic nature of L-glutamic dehydrogenase of higher plants. *Nature*, 207(993), 193–194.
- Titus, J.S. & Kang, S.-M. (1982) Nitrogen metabolism, translocation and recycling in apple trees. *Horticultural Reviews*, 4, 204–246.
- Turano, F.J., Dashner, R., Upadhyaya, A. & Caldwell, C.R. (1996) Purification of mitochondrial glutamate dehydrogenase from dark-grown soybean seedlings. *Plant Physiology*, 112(3), 1357–1364.
- Turano, F.J., Thakkar, S.S., Fang, T. & Weisemann, J.M. (1997) Characterization and expression of NAD(H)-dependent glutamate dehydrogenase genes in Arabidopsis. *Plant Physiology*, 113(4), 1329–1341.
- Watanabe, M., Itho, Y., Jo, Y., Yasuda, K., Kamachi, K. & Watanabe, Y. (2007) Redox and translational regulation of glutamate dehydrogenase a subunits in *Brassica napus* under wounding stress. *Plant Science*, 172(6), 1182–1192.
- Wen, Y., Yuan, X., Qin, F., Zhao, L. & Xiong, Z. (2019) Development and validation of a hydrophilic interaction ultra-high-performance liquid chromatography–tandem mass spectrometry method for rapid simultaneous determination of 19 free amino acids in rat plasma and urine. *Biomedical Chromatography*, 33(1), e4387.
- Yamada, K., Lim, J., Dale, J.M. et al. (2003) Empirical analysis of transcriptional activity in the Arabidopsis genome. *Science*, 302(5646), 842–846.
- Yaronskaya, E., Vershilovskaya, I., Poers, Y., Alawady, A.E., Averina, N. & Grimm, B. (2006) Cytokinin effects on tetrapyrrole biosynthesis and photosynthetic activity in barley seedlings. *Planta*, 224, 700–709.

SUPPORTING INFORMATION

Additional supporting information can be found online in the Supporting Information section at the end of this article.

How to cite this article: Brambilla, M., Chiari, G., Commisso, M., Nerva, L., Musetti, R., Petraglia, A. et al. (2023) Glutamate dehydrogenase in “Liverworld”—A study in selected species to explore a key enzyme of plant primary metabolism in Marchantiophyta. *Physiologia Plantarum*, 175(6), e14071. Available from: <https://doi.org/10.1111/ppl.14071>